ChemPubSoc Europe

DOI: 10.1002/chem.201304234

CHEMISTRY
A European Journal
Full Paper

Bisphosphines

New Functional Cyclic Aminomethylphosphine Ligands for the Construction of Catalysts for Electrochemical Hydrogen Transformations

Elvira I. Musina,*[a] Vera V. Khrizanforova,[a] Igor D. Strelnik,[a] Murad I. Valitov,[a] Yulia S. Spiridonova,[a] Dmitry B. Krivolapov,[a] Igor A. Litvinov,[a] Marsil K. Kadirov,[a] Peter Lönnecke,[b] Evamarie Hey-Hawkins,[b] Yulia H. Budnikova,[a] Andrey A. Karasik,[a] and Oleg G. Sinyashin[a]

Abstract: Eight-membered cyclic functional bisphosphines, namely 1,5-di-aryl-3,7-di(2-pyridyl)-1,5-diaza-3,7-diphosphacyclooctanes (aryl = 2-pyridyl, *m*-tolyl, *p*-tolyl, diphenylmethyl, benzyl, (*R*)-(+)-(α-methyl)benzyl), with 2-pyridyl substituents on the phosphorus atoms have been synthesized by condensation of 2-pyridylphosphine, formaldehyde, and the corresponding primary amine. The structures of some of these bisphosphines have been investigated by X-ray crystallography. The bisphosphines readily form neutral P,P-chelate complexes $[(\kappa^2\text{-P,P-L})MCl_2]$, cationic bis-P,P-chelate complexes $[(\kappa^2\text{-P,P-L})_2M]^{2+}$, or a five-coordinate complex $[(\kappa^2\text{-P,P-L})_2NiBr]Br$. The electrochemical behavior of two of the nickel complexes, and their catalytic activities in electrochemical hydrogen evolution and hydrogen oxidation, including the fuel-cell test, have been studied.

Introduction

Pyridylphosphines are multifunctional ligands which have the ability to act as hybrid P,N-ligands, as well pyridyl functionalized phosphines. The different donor abilities of phosphorus and nitrogen in pyridylphosphines as hybrid ligands reflects their versatile coordination behavior, which has been harnessed in precatalysts for a variety of processes,[1] for example, Pd-catalyzed hydrocarboxylation of acetylene[2] or oxidative carbonylation of phenol,[3] Ni-catalyzed olefin oligomerization,[4–6] Ru-catalyzed hydrogenation of bicarbonate[7] and ketones,[8] and Fe-mediated atom-transfer radical styrene polymerization.[9,10] Moreover, the ability of the phosphorus and nitrogen atoms of pyridyl diphosphine to form coordinate bonds to Cu^{I} has recently been used in the self-assembly of metal–organic frameworks (MOFs).[11]

Complexes of pyridylphosphines with a noncoordinated nitrogen atom from the pyridyl substituent are examples of functionalized systems in which the pyridyl group exhibits basic properties and is capable of secondary interactions, such as hydrogen bonding or proton transfer in the coordination sphere.[12] The ability of the pendant pyridyl groups to interact with weak proton donors suggests the possibility for use of the hydride complexes as catalyst precursors for a number of transformations in polar media, such as nitrile hydration reactions.[13,14] Protonation of the pyridyl group leads to increased water solubility of the corresponding metal complexes and can explain the enzyme-like catalytic activity of the Ru^{II} complexes in the hydration of terminal alkynes.[12,15,16]

On the other hand, cyclic aminomethylphosphines are compounds with phosphorus and nitrogen atoms incorporated into one cyclic system, such that these atoms influence one another. Despite the presence of two different heteroatoms, this system is not a hybrid ligand because the nitrogen atom is not usually coordinated,[17–19] but rather acts as pendant amine in the secondary coordination sphere of the corresponding metal.[20,21] Recently, the catalytic activity of Pd^{II} complexes of 1,5,3,7-diazadiphosphacyclooctanes for Suzuki–Miyaura cross-coupling in neat water without additional phase-transfer reagent was demonstrated.[22] Moreover, it has been shown that Ni^{II} complexes of some cyclic aminomethylphosphines (1,5-diaza-3,7-diphosphcyclooctanes and 1-aza-3,7-diphosphacycloheptanes) are the fastest synthetic catalysts known to date for hydrogen production[21,23] and oxidation,[24] reduction of oxygen,[25] and electrocatalytic oxidation of formate.[26] Reversible catalysis has been demonstrated for these catalysts in solu-

[a] *Dr. E. I. Musina, V. V. Khrizanforova, I. D. Strelnik, M. I. Valitov, Y. S. Spiridonova, Dr. D. B. Krivolapov, Dr. I. A. Litvinov, Dr. M. K. Kadirov, Prof. Dr. Y. H. Budnikova, Prof. Dr. A. A. Karasik, Prof. Dr. O. G. Sinyashin*
A. E. Arbuzov Institute of Organic and Physical Chemistry
Russian Academy of Sciences, Kazan Scientific Center
Arbuzov str. 8, 420088 Kazan (Russian Federation)
Fax: (+7) 8432752253
E-mail: elli@iopc.ru

[b] *Dr. P. Lönnecke, Prof. Dr. E. Hey-Hawkins*
Institut für Anorganische Chemie
Universität Leipzig
Johannisallee 29
04103 Leipzig (Germany)

Supporting information for this article is available on the WWW under http://dx.doi.org/10.1002/chem.201304234.

tion[27] and on modified electrodes.[28] The mechanism of hydrogen production/oxidation and the role of proton delivery and removal in these processes have been studied in detail.[29] It has been shown that the electronic and steric properties of substituents on both phosphorus and nitrogen can be used to tune these catalysts.[30]

Various cyclic and macrocyclic aminomethylphosphines with a variety of properties have been obtained by using diverse primary or secondary phosphines, aldehydes, and primary or secondary amines in a Mannich-like condensation reaction.[31] The substituents on the phosphorus atoms included aryl (phenyl,[23f,26,32] mesityl,[33] 2,4,6-tri-isopropylphenyl)[33], alkyl (methyl,[32b] *tert*-butyl,[34] cyclohexyl,[24,29a] menthyl,[35] butyl, 2,4-dimethylpentyl,[30] and benzyl),[30,36] ferrocenyl,[37] and ferrocenylmethyl[38] groups. However, only a few examples of aminomethylphosphines with functionalized substituents on the phosphorus atoms were derived from *ortho*-phosphinophenol.[39]

In the present work, we designed new pyridylphosphines based on the cyclic aminomethylphosphine platform to combine the properties of two systems—pyridylphosphine and aminomethylphosphine. The introduction of *ortho*-pyridyl substituents should expand the coordination modes of these ligands by introduction of an additional intramolecular pendant base situated in close proximity to the first coordination sphere of the corresponding transition metal and provide possibilities for nucleophilic activation of hydrogen in the course of electrochemical H_2 production or hydrogen oxidation in fuel cells.

Herein, we report the synthesis and crystal structures of several 1,5-diaza-3,7-diphosphacyclooctanes with *ortho*-pyridyl substituents on the phosphorus atoms, their neutral P,P-chelate complexes with platinum(II), palladium(II), and tungsten(0), and their cationic bis-P,P-chelate complexes with platinum(II), palladium(II), and nickel(II). The catalytic activity of the cationic nickel(II) bis-P,P-chelate complexes in electrochemical hydrogen evolution and the changes to the power density of a micro fuel cell with the complexes introduced into the near-electrode layer will be discussed.

Results and Discussion

Preparation and characterization of 1,5-diaza-3,7-diphosphacyclooctanes

2-Pyridylphosphine was synthesized by conventional reduction of diethyl-(2-pyridyl)phosphonate with $LiAlH_4$ (Scheme 1).[40] Diethyl-(2-pyridyl)phosphonate was obtained by an improved method[41] from *N*-pyridyl oxide, dimethyl sulfate, and diethylphosphite.

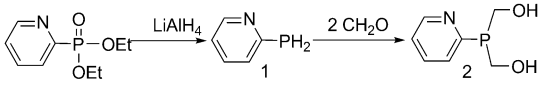

Scheme 1. Synthesis of bis(hydroxymethyl)(2-pyridyl)phosphine (**2**).

The reaction of pyridylphosphine (**1**) with paraformaldehyde at 100–105 °C led to bis(hydroxymethyl)(2-pyridyl)phosphine (**2**) as a viscous oil. According to $^{31}P\{H\}$ and ^{1}H NMR spectroscopy compound **2** was obtained with 90% purity and was used without purification. Condensation reactions of **2** with primary amines, namely 2-pyridylamine, *m*- and *p*-toluidine, diphenylmethylamine, benzylamine, and (*R*)-(+)-methylbenzylamine in ethanol at 60–70 °C led to the air-stable crystalline products **3**–**8**, respectively (Scheme 2). Compounds **3**–**5** are soluble in common organic solvents (benzene, chloroform, acetone, and DMF), **6a** and **8a** are less soluble, and **7a** is only soluble in hot DMSO.

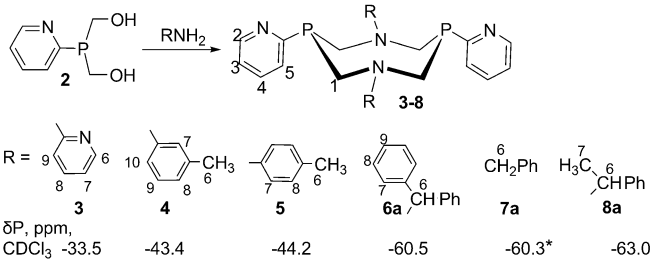

Scheme 2. Synthesis of 1,5,3,7-diazadiphosphacyclooctanes **3**–**8**. *$^{31}P\{H\}$ NMR spectrum of **7** was recorded in [D_6]DMSO.

$^{31}P\{H\}$ NMR spectra of compounds **3**–**8** showed one signal in the range $\delta = -33$ to -63 ppm. The chemical shifts strongly depend on the nature of the substituent at the nitrogen atom and are shifted to low field in the order: $CH(CH_3)Ph <$ benzyl $<$ CH(Ph)Ph $<$ *p*-tolyl $<$ *m*-tolyl $<$ 2-pyridyl. Diazadiphosphacyclooctane **3**, with a strong electron-withdrawing 2-pyridyl substituent on the nitrogen atom, showed a signal at $\delta = -33$ ppm, whereas analogous compounds **4** and **5**, with weak electron-withdrawing aryl substituents, showed a signal at $\delta \approx -44$ ppm, and compounds **6**–**8**, with electron-donating benzyl groups, have broad signals at $\delta \approx -60$ ppm. In addition, the yield also depends on the nature of the nitrogen substituents. The best yields (75–85%) were obtained for aryl-substituted heterocycles **4** and **5**, moderate yields (50–63%) for benzyl-substituted compounds **6a**–**8a**, whereas compound **3** was only obtained in low yield (20%), perhaps due to the low nucleophilicity of 2-pyridylamine. In the case of the benzyl-substituted amines, the six-membered 1,3-diaza-5-phosphacyclohexanes **6b** and **8b** were isolated as byproducts in 8% and 3% yield, respectively. The analogous heterocycle **7b** was detected in the reaction mixture by $^{31}P\{H\}$ NMR spectroscopy (Scheme 3). The formation of six-membered heterocycles was observed earlier for some Mannich-type condensation reactions between primary phosphines, formaldehyde, and primary amines.[38,39]

The signals of **6b**–**8b** in the $^{31}P\{H\}$ NMR spectra ($\delta = -58.2$, -52.5, and -58.1 ppm for **6b**, **7b**, and **8b**, respectively) are observed at slightly lower field than those of the corresponding diazadiphosphacyclooctanes.

The ^{1}H NMR spectra of compounds **3**–**5** in $CDCl_3$ show similar patterns for the heterocyclic methylene protons. The pro-

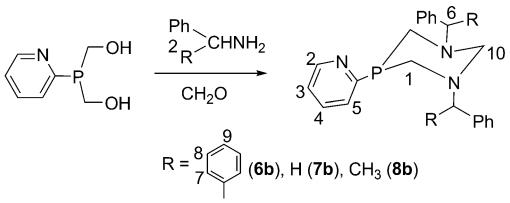

Scheme 3. The formation of six-membered heterocycles as co-products.

tons of the P–CH_2–N fragments appear as an ABX system and reveal inequivalence of the two diastereotopic hydrogen atoms. A notable difference in the values of the ^2J(P,H) coupling constants ($^2J(P,H)_A \approx 5$ Hz, $^2J(P,H)_B \approx 7$–15 Hz) was observed. This pattern is typical for diazadiphosphacylcooctanes in the crown conformation with a diaxial orientation of the lone pairs of electrons of the phosphorus atoms.[42] For **6a** in $CDCl_3$ and **7a** in DMSO these protons are observed as two doublets or a broad singlet, respectively. The heterocyclic methylene groups in **8a** are inequivalent in the ^{1}H NMR spectrum due to the presence of chiral substituents at the 1- and 5-positions of the heterocycle and form two (AA′)X spin systems, already observed for 1,5-diaza-3,7-diphosphacyclooctanes with chiral exocyclic substituents.[32d,37] The *m*-pyridyl protons H-5 and H-3 (numbering is shown in Scheme 2) of the benzyl-substituted diazadiphosphacyclooctanes **6a**–**8a** were observed at higher field ($\delta = 6.30$–7.20 ppm) than in the corresponding diazaphosphacyclohexanes **6b** and **8b** ($\delta = 7.12$–7.44 ppm). X-ray structure analyses of compounds **3**–**5**, **7a**, and **8a** were performed and confirmed the proposed structures. The crystal structures of **5** and **7a** are shown in Figures 1

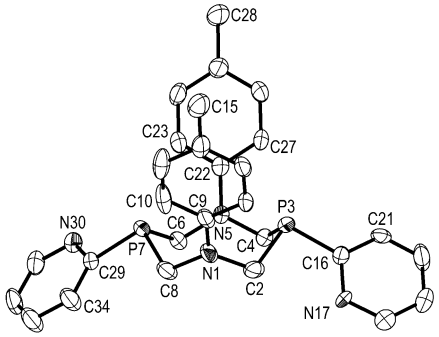

Figure 1. Molecular structure of **5**. The noncoordinating toluene molecule is omitted for clarity.

and 2. Crystals of compounds **3**, **4**, and **7a** contain only the said molecules, but **5** and **8a** crystallize with toluene and benzene, respectively (solvate molecule is disordered). The heterocyclic molecules have a crown (chair–chair) conformation with equatorial orientation of both *P*-pyridyl groups and a *syn* orientation of the lone pairs of electrons on phosphorus, suitable for metal chelation. The nitrogen atoms of compounds **3**–**5** with aromatic substituents are in an almost planar environment (the sum of the bond angles is 359.6(9), 358.6(5), and

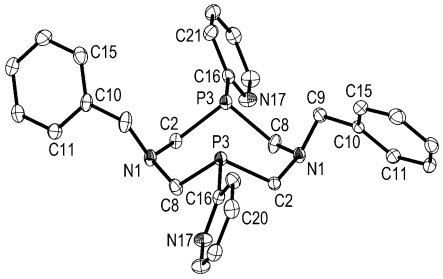

Figure 2. Molecular structure of **7a**.

359.7(4)°, respectively) (Figure 1), whereas for compounds **7a** and **8a**, the nitrogen atoms bonded to sp^3-carbon atoms are trigonal pyramidal (the sum of the bond angles is 340.3(4) and 340.7(4)°, respectively; Figure 2). The orientation of the *P*-pyridyl groups varies from orthogonal to parallel relative to the plane of the heterocycle.

Preparation of platinum, palladium, nickel, and tungsten complexes

It has been shown previously that 1,5-diaza-3,7-diphosphacyclooctanes readily form chelate complexes with group 10 transition metals.[23a,b,32d,35,38,39] Furthermore, the heterocyclic backbone of **3**–**8** resembles that of previously described ligands that contain two noncoordinating pendant amines, which function as proton relays in the corresponding Ni^{II} complexes, and dramatically increase the rates of intra- and inter-molecular proton transfer and assist in heterolytic cleavage/formation of the H–H bond.[20,21] As a result, complexes that contain these pendant bases are much faster electrocatalysts for both H_2 production and oxidation and operate at much lower overpotentials than analogous complexes without pendant amines.[23–26,43] The ligands with *P*-pyridyl substituents have additional coordination or pendant basic sites and, therefore, can either act as P,N-chelates or P,P-chelates with cyclic and exocyclic pendant bases capable of secondary interactions, such as hydrogen bonding or proton transfer. Ligands **5**, **7a**, and **8a** were chosen as typical representatives of 1,5,3,7-diazadiphosphacyclooctanes with aryl-, benzyl, and chiral substituents on the nitrogen atoms. We studied the coordination properties of the pyridyl-containing 1,5,3,7-diazadiphosphcyclooctanes described above to group 10 transition metals Ni^{II}, Pd^{II}, and Pt^{II}, which display similar behavior towards diphosphine ligands and prefer to adopt square-planar or tetrahedral coordination geometries. These d metals were supplemented by a tungsten(0)–carbonyl system that preferred octahedral coordination and was suitable for P,N-chelation in *fac*-P,P,N-complexes. 3,7-Di(2-pyridyl)-1,5-diaza-3,7-diphosphacyclooctanes **5**, **7a**, and **8a** readily react with [$PtCl_2$(cod)], [$PdCl_2$(cod)] (cod = 1,5-cyclooctadiene), [$NiBr_2$(dme)] (dme = dimethoxyethane), and [Ni($CH_3CN)_6$][BF_4]$_2$ as bidentate ligands to form mononuclear neutral P,P-chelate complexes **9**–**11** (Scheme 4) or cationic bis-P,P-chelate complexes **12**–**17**, dependent on the M/L ratio employed (Scheme 5). Ligand **5** forms also a stable P,P-chelate complex **18** with [$W(CO)_4$(cod)] (Scheme 4). Table 1 summarizes

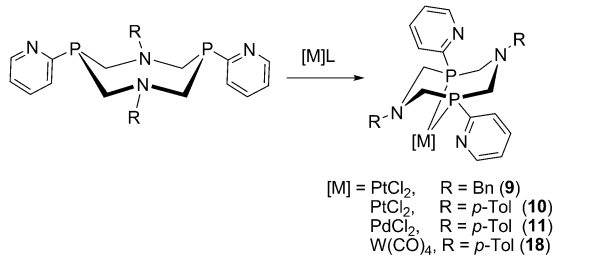

[M] = $PtCl_2$, R = Bn (**9**)
$PtCl_2$, R = *p*-Tol (**10**)
$PdCl_2$, R = *p*-Tol (**11**)
$W(CO)_4$, R = *p*-Tol (**18**)

Scheme 4. Synthesis of complexes **9**–**11** and **18**.

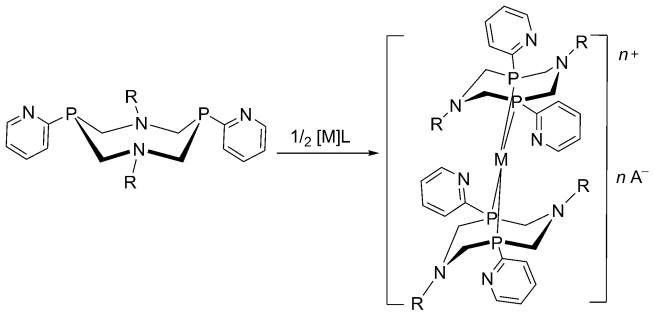

M = Pt, A = Cl, *n* = 2, R = *p*-Tol (**12**)
M = Pd, A = Cl, *n* = 2, R = *p*-Tol (**13**)
M = Pt, A = Cl, *n* = 2, R = CH_3(CH)Ph (**14**)
M = NiBr, A = Br, *n* = 1, R = *p*-Tol (**15**)
M = Ni, A = BF_4, *n* = 2, R = *p*-Tol (**16**)
M = Ni, A = BF_4, *n* = 2, R = CH_3(CH)Ph (**17**)

Scheme 5. Synthesis of complexes **12**–**17**.

the ^{31}P NMR spectroscopic data for complexes **9**–**18**. Compared to the free ligand, the signals for complexes **9**–**14** and **16**–**18** are shifted downfield ($\Delta\delta$ = 30–50 ppm), consistent with the reported deshielding of the P nuclei in six-membered chelate rings.[44]

The ^1J(P,Pt) values for complexes **9** and **10** (J = 2910 and 3054 Hz, respectively) and **12** and **14** (J = 2242 and 2259 Hz, respectively) are in the range expected for P nuclei in a *cis* and *trans* orientation, respectively. The presence of two broad bands in the FTIR spectra for the M–Cl vibrations ($\tilde{\nu}$ = 290 and 317 cm^{-1} for **10**; $\tilde{\nu}$ = 282 and 296 cm^{-1} for **11**) is further evidence of square-planar coordination with a *cis* orientation of the chloro ligands. Four carbonyl bands are observed at $\tilde{\nu}$ = 2014, 1920, 1902, and 1863 cm^{-1} for **18**, which is also consistent with the formation of a tetracarbonyl bisphosphine chelate complex.

Table 1. ^{31}P{H} NMR spectroscopic data of complexes **9**–**18**.

	Solvent	δ^{31}P [ppm]	$\Delta\delta$ [ppm][a]	^1J(M,P) [Hz]
9	$CDCl_3$	−24.2	36.1	2910[b]
10	$CDCl_3$	−12.5	31.8	3054[b]
11	$CDCl_3$	3.5	47.7	–
12	CD_2Cl_2	−15.4	28.8	2274[b]
12	$CDCl_3$	−14.3	30.0	2242[b]
12	D_2O	−14.8	29.4	2082[b]
13	$CDCl_3$	−0.6	43.7	–
13	D_2O	−9.8	34.5	–
14	$CDCl_3$	−11.7	51.4	2259[b]
14	D_2O	−10.8	52.3	2096[b]
15	CD_3CN	−11.4, 35.9	–	–
16	CD_3CN	0.7	43.5	–
17	CD_3CN	5.4	49.6	–
18	$CDCl_3$	2.62	46.9	204[c]

[a] $\Delta\delta = \delta_{ligand} - \delta_{complex}$. [b] M = Pt. [c] M = W.

The ABX spin system produced by the protons of the P–CH_2–N fragments of **9**–**18** is observed as two complex multiplets in the ^{1}H NMR spectra. Interestingly, in complex **12** (in $CDCl_3$ or CD_2Cl_2) one of the protons of the P–CH_2–N fragment is observed as a doublet with ^3J(Pt,H) satellites (^3J(Pt,H) = 42.2 Hz). The platinum and palladium complexes **12**–**14** are highly soluble in water due to the presence of four pyridyl groups and the ionic structure. The chemical shifts of **12** and **14** in the ^{31}P{H} NMR spectra in D_2O and $CDCl_3$ are similar but the ^1J(Pt,P) coupling constants are approximately 150 Hz lower in D_2O (Table 1)

The phosphorus signal of the Pd complex **13** in D_2O was shifted upfield compared to $CDCl_3$ (δ = −9.8 ppm). In D_2O, only one broad singlet is observed for the protons of the P–CH_2–N fragment. In contrast to **12**–**14**, the ^{31}P{H} NMR spectra of nickel(II) complex **15** showed two multiplets of an AA′XX′ spin system at δ = −11.4 and 35.9 ppm, which indicates the inequivalence of the phosphorus atoms in this complex, possibly due to a d^8 low-spin five-coordinate nickel(II) ion with trigonal-bipyramidal coordination as described for $[NiCl(PMe_3)_4]Cl$[45] (two triplets at δ = −1.5 and +28.6 ppm, J(P,P) = 79 Hz, at 114 K), which exhibits axial–equatorial exchange of the PMe_3 groups. The exchange rate of **15** is much lower than that of $[NiCl(PMe_3)_4][Cl]$ due to presence of chelate cyclic bisphosphines. MALDI mass spectrometry (m/z: 1107, $[M-Br]^+$) confirmed the formation of the cationic five-coordinate nickel(II) complex $[NiBrL_2][Br]$. In the case of the four-coordinate nickel complexes **16** and **17**, with tetrafluoroborate as the counterion, all four phosphorus atoms are equivalent in the ^{31}P{H} NMR spectra (**16**: δ = 0.7 ppm, *s*; **17**: δ = 5.4 ppm, *s*).

The model five-coordinate nickel(II) complex $[(\kappa^2\text{-P,P-L})_2NiCl][Cl]$ (**19**), in which L = 1,3,5,7-tetraphenyl-1,5-diaza-3,7-diphosphacyclooctane, was synthesized from 1,3,5,7-tetraphenyl-1,5-diaza-3,7-diphosphacyclooctane and $NiCl_2$. MALDI mass spectrometry (m/z: 1003, $[M-Cl]^+$) confirmed the formation of the cationic five-coordinate nickel(II) complex $[NiClL_2]Cl$. The NMR spectra of **19** are similar to those of **15** and show two multiplets at δ = −14.0 and 21.6 ppm, which demonstrated the analogous structures of both complexes in solution.

Molecular structures of transition-metal bisphosphine complexes

The molecular structures of the neutral monochelate complexes **10**, **11**, and **18** and cationic bis-P,P-chelate complexes **12**, **13**, and **16** were unambiguously established by X-ray crystallography. Complexes **10** and **11** are very similar and show square-planar geometry around the metal center with a *cis* arrangement of the two coordinating Cl atoms (Figure 3). The P-M-P bite angles are 83.5(2) (**10**) and 82.7(4)° (**11**).

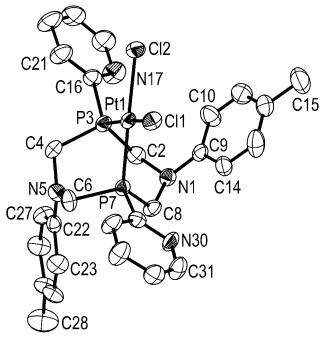

Figure 3. Molecular structure of **10**. Solvent molecules are omitted for clarity.

The heterocyclic ligands in **10** and **11** have a different conformation than the chair–chair conformation of the free heterocycle (**5**). The metal atoms are included in the bicyclic (bicyclononane) system, so the conformation may be analyzed as two six-membered metallacycles: one of them has a chair conformation, the other has a boat conformation. The N1 nitrogen atom of the boat part of the heterocycle is nearly trigonal pyramidal (sum of C-N-C bond angles are 346.4(2) and 347.6(2)° for **10** and **11**, respectively) and is in close proximity to the metal center (Pt···N1 = 3.317 Å, Pd···N1 = 3.280 Å, sum of the van der Waals radii = 3.27 and 3.18 Å,[46] respectively). The N5 nitrogen atom in the chair part of the molecule is trigonal planar in **10** (sum of C-N-C bond angles is 359.6(2)°), and trigonal pyramidal in **11** (sum of C-N-C bond angles is 345.0(2)°). The pyridyl group on the phosphorus atom P7 is nearly orthogonal to the MP_2Cl_2 plane (dihedral angles: 75.9° for **10** and 86.8° for **11**). Thus, the pyridyl N atoms located above or below the MP_2Cl_2 plane are suitable for controlling the direction of incoming substrates.

Crystals of the P,P-chelate tungsten complex **18** were obtained by slow diffusion of *n*-hexane into a solution of **18** in $CDCl_3$. Complex **18** represents an example of a distorted octahedral 1,5-diaza-3,7-diphosphacyclooctane complex (P3–W–P7 = 73.70(2)°). The average W–P bond length (2.4779(8) Å) is slightly shorter than that typical for P,P-chelate complexes of tungsten(0) (2.50–2.52 Å).[47] A chair–boat conformation of the ligand is observed in **18** (Figure 4), similar to the conformation

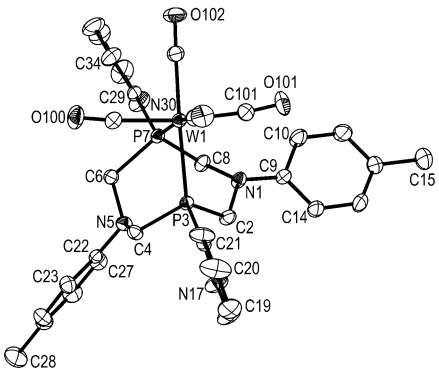

Figure 4. Molecular structure of **18**.

of complexes of group 10 metals. The environment of the intracyclic nitrogen atom N1 of the boat part of the bicyclononane system is nearly planar (sum of bond angles is 353.4(3)°). In the chair part the N5 atom is nearly pyramidal (sum of bond angles is 344.4(2)°). The bond lengths N5–C_{exo} and N1–C_{exo} (1.434(4) and 1.412(4) Å, respectively) correlate with the coordination of the nitrogen atoms. The average bond length observed for the W–C(carbonyl) bond *trans* to the phosphorus atom (1.994(3) Å) is shorter than that of common bisphosphine complexes (2.029(4) Å on average).[47]

Crystals of the cationic bis(P,P)-chelate complexes **12** and **13** were grown by slow evaporation from solutions in chloroform. Crystals of the corresponding nickel complex **16** were obtained by slow diffusion of ethanol into a solution of **16** in acetone. The molecular structures of **12**, **13**, and **16** consist of discrete cations formed by two bisphosphine ligands and platinum(II), palladium(II), or nickel(II) and two noncoordinating chloride (**12** and **13**) or tetrafluoroborate (**16**) anions. Cations of the complexes **12** and **13** are isostructural. The platinum and palladium atoms are located on a crystallographic twofold axis. The symmetry independent part of the molecule contains one chelate ligand. The molecular structures of the cations **13** and **16** are shown in Figures 5 and 6.

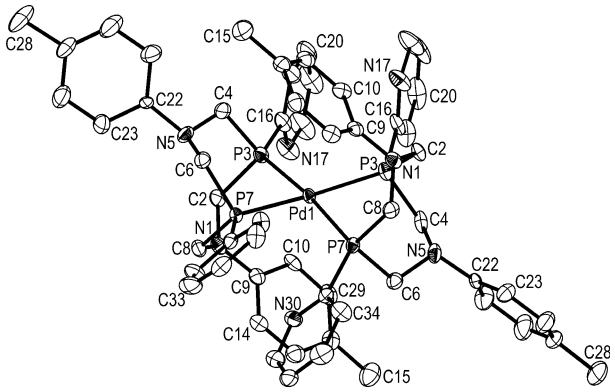

Figure 5. Molecular structure of the cation of **13**. Counterions and solvate molecules are omitted for clarity. The corresponding Pt complex **12** is isostructural.

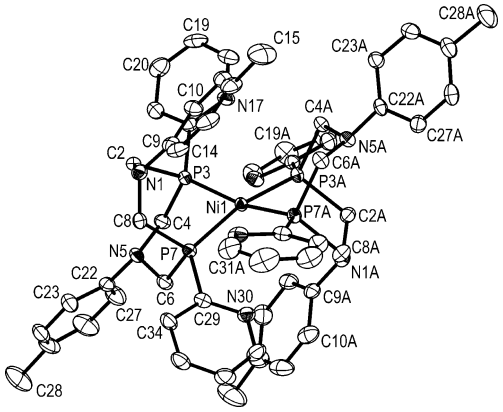

Figure 6. Molecular structure of the cation of **16**. Counterions and solvate molecules are omitted for clarity.

In contrast to complexes **10** and **11**, complexes **12**, **13**, and **16** exhibit a slightly (**12**, **13**) or noticeably (**16**) distorted square-planar geometry around the metal center. The dihedral angle between the P3-M1-P7 and P3A-M1-P7A planes is 10.0° for **12**, 10.5° for **13**, and 22.9° for **16**. The Pt–P bond lengths are typical for platinum(II) complexes with similar bidentate phosphine ligands.[17] The P-M-P bond angles of 81.4(1), 81.62(6), and 84.36(4)° for **12**, **13**, and **16** are slightly smaller than those of linear bisphosphines.[17,48] Both heterocyclic ligands of the complexes **12**, **13**, and **16** have a chair–boat conformation. The N1 nitrogen atom of the boat part of the heterocycle is close to the metal center (Pt···N1 = 3.319 Å in **12**, Pd···N1 = 3.330 Å in **13**, and Ni···N1 and Ni···N1A = 3.371 and 3.394 Å in **16**. The geometry is nearly trigonal planar in **12** and **13** (sum of C-N1-C bond angles is 353.0 and 351.8°, respectively) and distorted trigonal pyramidal in **16** (sum of C-N1-C and C-N1A-C bond angles is 347.1 and 347.9°). The remote nitrogen atom N5 of the chair part has a trigonal pyramidal configuration (sum of bond angles is 342.1° for **12**, 339.8° for **13**, and 339.5 and 343.3° for **16**). The *P*-pyridyl substituents of **12** and **13** are arranged in a nearly parallel fashion (dihedral angles between the planes of close pyridyl rings are 23.9 and 6.0° for **12** and 23.2 and 3.6° for **13**). The distance between the centroids of the pyridyl rings is approximately 3.45 Å. Two pyridyl groups are nearly orthogonal to the MP_4 plane (dihedral angles are 85.0° in **12** and 87.6° in **13**) with the basic nitrogen atom located above and below this plane. In **16**, all pyridyl groups have dihedral angles with the NiP_4 plane that vary from 31.8–45.2°. Unlike the structure of Ni^{II} complexes with phenyl groups on phosphorus,[23a] in which both nitrogen atoms in the boat part of the ligands are located on one side relative to the medium NiP_4 plane, in **16** these nitrogen atoms are located on opposite sides relative to this plane. As a result, the BF_4 counterion in *P*-phenyl substituted complexes is close to the nickel ion,[23a] whereas in **16** it is remote from the cation.

Single crystals of complex **15** suitable for X-ray structure analysis could not be obtained, but single crystals of model complex **19** were obtained by slow evaporation of its solution in chloroform. The compound crystallizes in the space group *C*2/*c* with eight molecules in the unit cell and confirmed the proposed trigonal bipyramidal structure of the cationic bis-chelate complex **19**, with chlorine and two phosphorus atoms of different chelate ligands in the equatorial positions and two phosphorus atoms in the axial positions (Figure 7).

The endocyclic amine groups of both ligands located in the chair parts of the chair–boat ligands point out towards the chloro ligand. In total, the structure of cation **19** is similar to one reported by Kilgore[23a] that contained the tetrafluoroborate anion proximal to the nickel center rather than coordinated chlorine. In summary, the molecular structures indicate that both the endo- and exo-cyclic basic sites of the ligands are located in close proximity to the first coordination sphere of the transition-metal complexes. Thus, both types of basic site have the potential to participate in hydrogen activation by the metal center or in proton transfer to the metal center in the course of an electrochemical oxidation or the production of hydrogen.

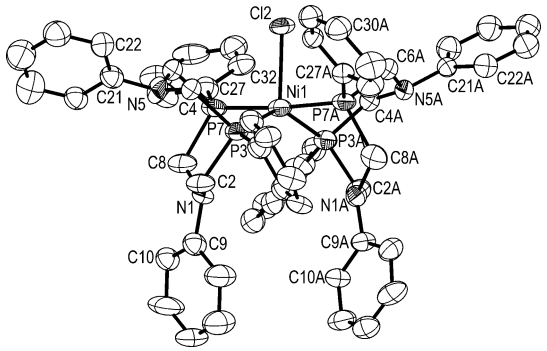

Figure 7. Molecular structure of **19**. Counterion is omitted for clarity.

Electrochemical studies of nickel complexes 16 and 17

It was found that the complexes of the type $[(\kappa^2\text{-P,P-L})_2Ni][BF_4]_2$ (**16** and **17**) are able to activate and oxidize hydrogen in the coordination sphere, similarly to hydrogenases[49] and to catalyze hydrogen evolution. Therefore, the electrochemical features of nickel complexes **16** and **17** were studied. It should be mentioned that the data obtained for the electrochemical reduction of complexes **16** and **17**, generated in situ from the corresponding ligand and $Ni(BF_4)_2$, are the same. Both nickel complexes **16** and **17** display two distinct reversible reduction waves with a peak-to-peak separation (ΔE_p) for each wave of 50–81 mV in acetonitrile (Table 2 and Figure 8; Figure S1 in the Supporting Information).

Table 2. Electrochemical data for nickel complexes **16** and **17** in acetonitrile.

	$E_{1/2}$ [V]	ΔEp [mV]	i_a/i_c[a]
	$Ni^{II/I}$		
16	−0.82	50	0.82
17	−0.90	81	0.86
	$Ni^{I/0}$		
16	−1.00	58	1.1
17	−1.12	58	1.1

[a] i_a = anodic current, i_c = cathodic current.

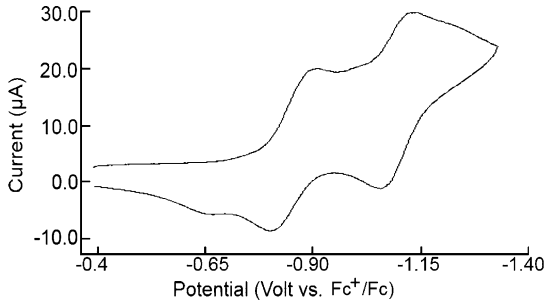

Figure 8. Cyclic voltammogram of a solution of **17** in acetonitrile (c = 1.5 mM). Conditions: scan rate = 0.1 $V s^{-1}$, Bu_4NBF_4 (0.1 M), glassy-carbon working electrode.

The two waves are assigned to the $Ni^{II/I}$ and $Ni^{I/0}$ couples. Plots of the peak current (i_p) versus the square root of the scan rate display linear relationships for both couples, which indicated that these redox processes are diffusion controlled (see the Supporting Information, Figure S2). Values of $E_{1/2}$ for the nickel(II/I) and nickel(I/0) couples range from $E_{1/2} = -0.82$ to -0.90 V and $E_{1/2} = -1.00$ to -1.12 V, respectively, and are comparable to that of the previously described analogues with *P*-phenyl and *P*-benzyl substituents.[23a, 30a]

Catalytic hydrogen production

The nickel complexes **16** and **17** were tested as electrocatalysts for hydrogen production. The electrocatalytic experiments were performed in dry CH_3CN with CF_3COOH as a proton source ($pK_a(CH_3CN) = 12.7$).[50] The H_2 production activity was measured by cyclic voltammetry (CV) of reaction mixtures for which the acid concentrations were systematically increased until the i_{cat}/i_p ratio remained constant—the acid-independent region (Figures 9 and 10 for **17**; see the Supporting Information, Figures S5 and S7 for **16**). The duration of these experiments was restricted to approximately 30 min and minimal (<5%) catalyst decomposition was observed, determined by UV/Vis spectroscopy for each complex (see the Supporting Information, Figure S3). Trace 1 in Figure 9 corresponds to the reduction of complex **17** in the absence of acid. The cyclic voltammograms represented in traces 2–7 (Figure 9) were recorded in the presence of increasing acid concentration. A significant increase in the current near the nickel(I/0) couple is detected as rising amounts of acid are added (Figure 9). The wave of the nickel(II/I) couple remained at constant current and was positively shifted by 50–100 mV in the presence of acid relative to the acid-free environment. The electrocatalysis occurs at a potential of -1.4 V for complex **16** and -1.5 V for complex **17**. We observed intensive gas evolution on the surface of the working electrode at these potentials. An analogous hydrogen evolution phenomenon has been described for nickel complexes of cyclic aminomethylphosphines.[23c] The catalytic enhancement at the $Ni^{I/0}$ reduction peak is not consistent with the catalytic cycle proposed for catalysts that contain *P*-phenyl or *P*-benzyl substituents; in these cases, a catalytic increase of current at the $Ni^{II/I}$ peak was observed.[23f, 49a]

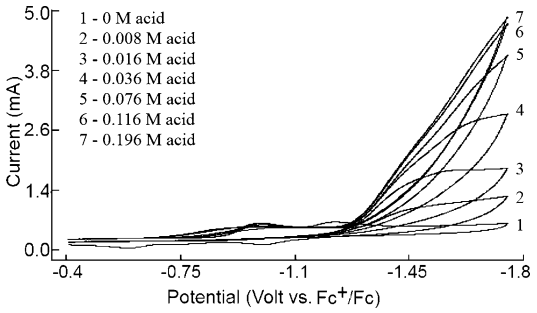

Figure 9. Cyclic voltammograms of solutions of **17** in acetonitrile ($c = 1.5$ mM) in the presence of various amounts of CF_3COOH. Conditions: scan rate = 10 V s^{-1}, $(Bu_4N)BF_4$ (0.1 M), glassy-carbon electrode.

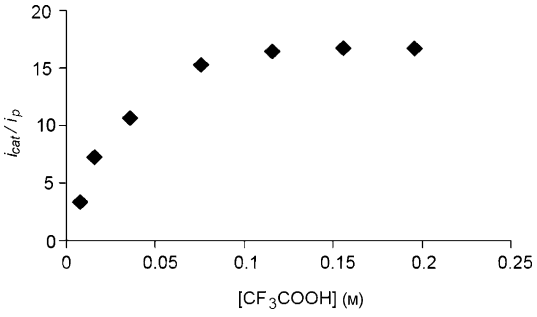

Figure 10. Plot of i_{cat}/i_p versus $[CF_3COOH]$ for **17** in acetonitrile.

Equation (1) [see the Experimental section] has been used to calculate a turnover frequency (TOF) of 3050 s^{-1} for **16** and 5200 s^{-1} for **17** in the acid-independent region. These results show that complexes **16** and **17**, with pyridyl-substituted ligands, display higher TOFs in organic media than the corresponding phenyl- and benzyl-substituted nickel complexes reported earlier.[23a,e,30,32e] However the overpotentials of catalysts **16** and **17**, calculated by the method of Evans et al.[51] range from 0.5–0.6 V for **16** and **17**, respectively (Table 3) and are slightly higher than for other complexes of this type.[23a,e,30,32e]

Table 3. Electrocatalytic data for hydrogen production.

	16	**17**
potential of catalysis [V]	−1.4	−1.5
$[CF_3COOH]$ [M]	0.14	0.11
k_{obs} [s^{-1}]	3050	5200
k [$M^{-1}s^{-1}$]	21 000	47 000
overpotential [V]	0.5	0.6

Probably, the increase of overpotential is caused primarily by current enhancement of the nickel(I/0) reduction peak in the catalytic process. Detailed determination of the reasons of the higher overpotential and the mechanism of H_2 production is outside the scope of this work and will be discussed at a future date.

The dependence of the catalytic current on catalyst concentration at a constant acid concentration has linear character (see Figure S6 in the Supporting Information). The second-order rate constants (first order in acid and first order in catalyst) were determined from plots of k_{obs} versus $[H^+]$ (Figure 11 for **17**; Figure S8 in the Supporting Information for **16**); $k =$ 21 000 and 47 000 $M^{-1}s^{-1}$ for **16** and **17**, respectively (Table 3). Thus, the catalytic activities of nickel complexes **16** and **17** for electrochemical hydrogen evolution in CH_3CN are rather high and are comparable to, or even better than, similar catalysts based on 1,5-diaza-3,7-diphosphcyclooctanes described to date.

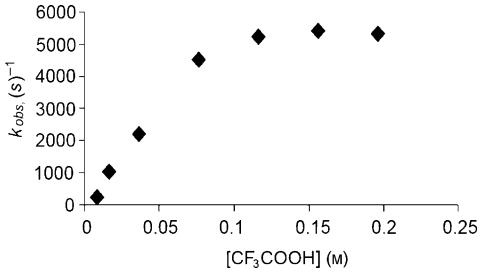

Figure 11. Plots of k_{obs} versus [CF_3COOH] for hydrogen evolution in acetonitrile catalyzed by **17**.

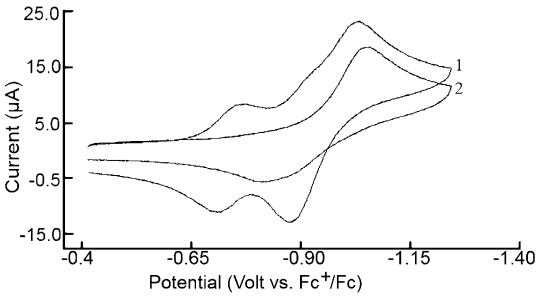

Figure 13. CV spectra of **16** in CH_3CN ($c = 2$ mM). Conditions: scan rate = 0.1 V s^{-1}, $(Bu_4N)BF_4$ (0.1 M). 1) Complex **16**, 2) complex **16** after exposure to H_2.

Fuel-cell tests

It has been demonstrated that hydrogen reacts with **17**. The red solution of **17** in CD_3CN became light yellow after exposure to a hydrogen flow for 1 h, and the ^{31}P NMR spectrum showed almost complete disappearance of the signal for complex **17** and the appearance of several new peaks in the range $\delta = 9.8$–16.1 ppm. Similar spectral changes have been described for the formation of protonated Ni^0 complexes as a result of the interaction of analogous Ni^{II} complexes with hydrogen.[23b,24] The presence of several signals indicates that a mixture of isomers is present, but the positions of the protons that resulted from the H_2 oxidation are not yet completely determined. It should be mentioned that the appearance of a peak at $\delta = 8.84$ ppm in the ^1H NMR spectrum suggests protonation of the pyridyl nitrogen centers and the endocyclic nitrogen atoms. The nearly complete disappearance of the initial peaks in the CV spectra of **17** after exposure to hydrogen was observed (Figure 12) and was consistent with the chemical reduction of **17** to the corresponding nickel(0) complex and concomitant hydrogen oxidation. In the case of **16**, two peaks in the CV spectra merged into one after hydrogen was passed through a solution of complex **16** in CH_3CN (Figure 13). The ^{31}P and ^1H NMR spectra of **16** were unchanged after exposure to a flow of hydrogen for several hours.

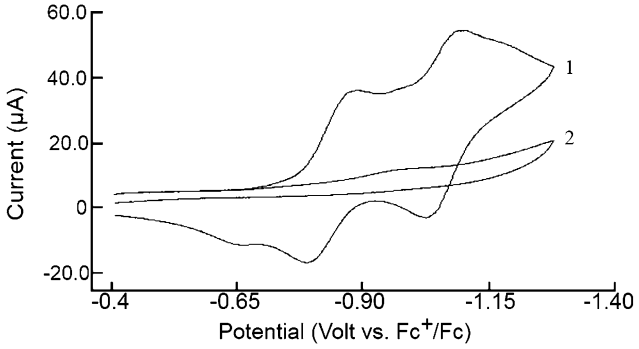

Figure 12. CV spectra of **17** in CH_3CN ($c = 2$ mM). Conditions: scan rate = 0.1 V s^{-1}, $(Bu_4N)BF_4$ (0.1 M). 1) complex **17**, 2) complex **17** after exposure to H_2.

The catalytic properties of **16** and **17** in the oxidation of hydrogen were investigated in a specially constructed miniature fuel cell (FC) [see the Supporting Information, Figure S11].[52] The aim of the experiments was to determine the influence of the introduction of solutions of **16** and **17** in dichloromethane at the anode side of the membrane-electrode assembly (MEA) on the power density of the FC (see the Experimental section and Supporting Information). Carbon-containing molecules (including CH_2Cl_2) in "cold combustion" in the FC are able to produce carbon monoxide, which contaminates the platinum catalyst and degrades the diagnostic characteristics. To reduce the negative impact of carbon monoxide contamination, we used a MEA with a platinum density of 4 mg cm^{-2}. The resultant diagnostic curves (power density versus current density; Figure 14; see the Supporting Information, Figure S12) demonstrate that treatment of the fuel cell with compound **16** or **17** improves the power density of the FC by 25–30 and 45-52%, respectively, when applied on the anode side in equal volumes of dichloromethane.

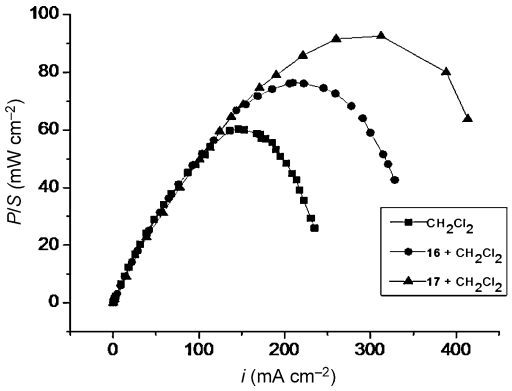

Figure 14. FC diagnostic curves with 4.0 mg cm^{-2} Pt/Nf MEA (Nf = Nafion) by addition of (■) CH_2Cl_2 (10 μL), (●) a solution of **16** in CH_2Cl_2 ($c = 5\times10^{-4}$ mol l^{-1}), and (▲) **17** in CH_2Cl_2 ($c = 5\times10^{-4}$ mol l^{-1}) at the anode side.

Conclusions

The reaction of 2-pyridylphosphine, formaldehyde, and various primary amines resulted in eight-membered cyclic pyridyl-substituted bisphosphines, the structures and coordination properties of which were similar to those of other 1,5-diaza-3,7-diphosphacyclooctanes. These ligands form mono-P,P-chelate and cationic bis-P,P-chelate complexes with group 10 transition

metals and tungsten(0). An important advantage to the introduction of a pyridyl substituent on the phosphorus atom of 1,5-diaza-3,7-diphosphacyclooctanes is the improved water solubility of the resultant transition-metal complexes, which makes them potentially useful for biphasic catalysis and applications in medicine. The nitrogen atoms of the pyridyl groups were not involved in coordination in the transition-metal-complex studies, even when an excess of the metal salt was used. However, they are located in close proximity to the first coordination sphere of the transition metal and participate as pendant bases in electrochemical hydrogen oxidation/evolution. The catalytic activity of the cationic bis-P,P-chelate complexes with nickel(II) in electrochemical hydrogen evolution is comparable to the best catalytic systems in organic media described to date. Finally, preliminary results indicate that introduction of the nickel complexes **16** and **17** into the near-electrode layer of a real fuel cell increased the power density by up to 52%.

Experimental Section

General

All reactions and manipulations were carried out under a dry argon atmosphere by using standard vacuum-line techniques. Solvents were purified, dried, deoxygenated, and distilled before use. EI-MS (70 eV) were recorded with a DFS Thermo Electron Corporation (Germany) spectrometer with direct sample admission into the ion source (ion-source temperature = 280 °C; vaporizer temperature programmed from 50–350 °C). The XCalibur program was used to process the mass spectrometry data. The mass spectra are reported as *m/z* values with relative intensities (I_{rel}) [%]. MALDI mass spectra were obtained with a Bruker ULTRAFLEX III mass spectrometer (Nd: YAG Smartbeam laser, $\lambda = 355$ nm) in a linear mode, without accumulation of mass spectra. ^{1}H NMR (400 MHz), ^{13}C NMR (101 MHz), and ^{31}P NMR (162 MHz) spectra were recorded with a Bruker Avance-DRX 400 spectrometer. Chemical shifts (δ) are reported in ppm relative to $SiMe_4$ (^{1}H, ^{13}C; internal standard) and 85% H_3PO_4 (aq) [^{31}P; external standard]. Coupling constants (*J*) are reported in Hz. Atom numbering is shown in Schemes 2 and 3. IR spectra were recorded on an FTIR spectrometer Tensor 27 (Bruker) in the range $\tilde{\nu} = 4000$–400 cm^{-1}, and far-IR spectra of solid samples in Nujol, placed between polyethylene plates, on an FTIR spectrometer IFS-66v/s (Bruker) in the range $\tilde{\nu} = 600$–100 cm^{-1}, both at an optical resolution of 4 cm^{-1}.

Electrochemical methods

CV measurements were performed with a BAS Epsilon (USA) E2P potentiostat comprised of a measuring block, Dell Optiplex 320 computer with installed Epsilon ES-USB-V200 program, and a C3 electrochemical cell. A stationary glassy-carbon electrode was used as the working electrode. A Fc^+/Fc (Fc = ferrocenyl) system served as the reference electrode. A platinum wire with a diameter of 0.5 mm was used as the auxiliary electrode. Measurements were performed under an argon atmosphere.

H_2 production measurements

A solution of the nickel complex (1.5 mM) in acetonitrile (5 mL) that contained $(Bu_4N)BF_4$ (0.1 M) was prepared. Nickel complexes were titrated with trifluoroacetic acid (TFA). Aliquots of acid were added by microsyringe (10 μL increments) until the catalytic current (i_{cat}) no longer increased. The catalytic current was measured at −1.4 and −1.5 V. The ratio of i_{cat}/i_p versus the acid concentration were plotted and the i_{cat}/i_p ratio in the acid-independent region was used to determine the catalytic rate constant according to Equation (1),[23c,53]

$$k_{obs} = \nu\left(\frac{i_{cat}/i_p}{0.72}\right) \quad (1)$$

in which k_{obs} is the observed rate constant, υ is the scan rate [V s^{-1}], and a two-electron process is assumed.

Fuel-cell (FC) tests

Diagnostic curves of the MEAs studied were measured with a gas-flow-controlling unit MTS-A-150 and potentiostat ESL 450 (both Electro Chem Co.) in a specially constructed miniature FC[52] (see the Supporting Information, Figure S11). The FC consists of two teflon half-cylinders. Gas-feeding channels inside each half-cylinder admit oxygen and hydrogen. The active part includes a Pt mesh spacer that allows gas distribution and at the same time provides electrical contact, and a MEA (the membrane with Pt electrodes deposited on both sides). Nafion 117 (Nf) manufactured by DuPont is available commercially. Platinum catalyst was deposited on the membrane from a suspension of platinum black particles with sizes of 30–50 nm in an aqueous solution of Nafion (5%). Platinum–Nafion (Pt/Nf) MEAs with platinum densities = 1, 2, and 4 mg cm^{-2} were fabricated by pressing for 7 min at 177 °C under a pressure of 35 atm. Experiments were carried out with a H_2/O_2 FC. The flow rate of hydrogen was 14 cm^3 min^{-1} and that of oxygen was 7 cm^3 min^{-1}. Diagnostic curves have been measured for the above-mentioned MEA and with the addition of a solution (5×10^{-4} mol l^{-1}; 10 μL) of the studied complexes at the anodic side. Each measurement was repeated (×3); see the Supporting Information.

X-ray crystallography

The X-ray data for **4**, **5**, and **7a** were collected on a Gemini diffractometer (Agilent Technologies) at $T = 130(2)$ K and the data for **3**, **8a**, **10**–**13**, **16**, **18**, and **19** were collected on Bruker Smart Apex II CCD diffractometer at $T = 296(2)$ [**3**, **11**, **13**, **18**, **19**], 293(2) [**8a**, **10**, **12**], and 150(2) K (**16**), by using $Mo_{K\alpha}$ radiation ($\lambda = 0.71073$ Å). Data reduction of **4**, **5**, and **7a** was performed with CrysAlis Pro software,[54] and included the program SCALE3 ABSPACK[55] for empirical absorption correction. Data reduction of **3**, **8a**, **10**–**13**, **16**, **18**, and **19** was performed with the APEX2[56] program, and included the program SAINT[56] and SADABS.[57] All structures were solved by direct methods[58,59] and refined with SHELXL-97.[59] Non-hydrogen atoms were refined with anisotropic thermal parameters, with the exception of the minor (17%) disordered part of the structure of **4**. Hydrogen atoms in **4**, CH_3 substituents, and disordered parts in **5** were calculated on idealized positions by using the riding model, whereas all other hydrogen atoms are located at the end of the structure refinement by using a difference-density Fourier map. Hydrogen atoms in **3**, **8a**, **10**–**13**, **16**, **18**, and **19** were refined as riding atoms. Structure representations were generated with DIAMOND-3.[60] The crystallographic data and summary of data collection and refinement are presented in Table S1 (see the Supporting Information).

CCDC-93002 (**3**), CCDC-932709 (**4**), CCDC-932710 (**5**), CCDC-932711 (**7a**), CCDC-933003 (**8a**), CCDC-932995 (**10**), CCDC-932996 (**11**),

CCDC-932997 (**12**), CCDC-932998 (**13**), CCDC-93299 (**16**). CCDC-933000 (**18**), and CCDC-93001 (**19**) contain the supplementary crystallographic data for this paper. These data can be obtained free of charge from The Cambridge Crystallographic Data Centre via www.ccdc.cam.ac.uk/data_request/cif.

Synthesis of starting materials

$[PtCl_2(cod)]$ was prepared from $H_2[PtCl_6]\cdot 6H_2O$ according to a modified procedure (see the Supporting Information).[61] $[PdCl_2(cod)]$,[62] $[Ni(NCMe)_6][BF_4]_2$,[63] and $[NiBr_2(dme)]$[64] were prepared by published procedures. $[W(CO)_4(cod)]$ was purchased from Aldrich. *O,O*-Diethyl(pyrid-2-yl)phosphonate was obtained from pyridine-*N*-oxide and sodium diethylphosphonate by an improved Redmors[41] method (see the Supporting Information). 2-Pyridylphosphine (**1**) was obtained from *O,O*-diethyl(pyrid-2-yl)phosphonate by reduction with $LiAlH_4$ in diethyl ether.[40]

Synthesis

Compound 2: A mixture of 2-pyridylphosphine (1.39 g, 12.5 mmol) and paraformaldehyde (0.75 g, 25.0 mmol) was stirred at 110 °C until homogenization was observed. ^{1}H NMR (400 MHz, $CDCl_3$): $\delta =$ 8.59 (d, $^3J(H,H) = 4.4$ Hz, 1H; H-2), 7.70 (dddd, $^3J(H,H) = 7.3$, 7.8 Hz, $^4J(H,H) \approx {}^4J(P,H) \approx 2$ Hz, 1H; H-4), 7.63 (ddd, $^3J(H,H) = 7.8$, 4.4 Hz, $^4J(H,H) \approx 2$ Hz, 1H; H-3), 7.28 (ddd, $^3J(H,H) = 7.3$ Hz, $^3J(P,H) \approx 4$ Hz, $^4J(H,H) \approx 2$ Hz, 1H; H-5), 5.59–4.95 (brm, 2H; OH), 4.63 (dd, $^2J(H,H) = 13.2$ Hz, $^2J(P,H) = 7.8$ Hz, 2H; H-1_A), 4.51 ppm (dd, $^2J(H,H) =$ 13.2 Hz, $^2J(P,H) = 10.8$ Hz, 2H; H-1_B); $^{31}P\{^1H\}$ NMR (162 MHz, $CDCl_3$): $\delta = -16.7$ ppm. Compound **2** was synthesized immediately before use.

Compound 3: Compound **2** (2.21 g, 12.9 mmol) was dissolved in dry ethanol (10 mL) and a solution of 2-pyridylamine (1.24 g, 13.2 mmol) in dry ethanol (7 mL) was added. The mixture was stirred at 70 °C for 72 h. The precipitate formed was filtered off, washed carefully with ethanol, and dried at 0.05 torr for 3 h. The filtrate was heated at 70 °C for 24 h and the precipitate formed was filtered off (×2). The combined precipitates were washed with ethanol and dried at 0.05 torr for 3 h to give **3** (0.6 g, 20%). Single crystals of **3** suitable for X-ray crystal structure analysis were obtained by recrystallisation of the crude product from ethanol. M.p. 196–198 °C; ^{1}H NMR (400 MHz, $CDCl_3$): $\delta = 8.71$ (ddd, $^3J(H,H) =$ 4.8 Hz, $^4J(H,H) = 2.0$ Hz, $^5J(H,H) = 1.0$ Hz, 2H; H-2), 8.19 (ddd, $^3J(H,H) = 4.9$ Hz, $^4J(H,H) = 1.9$ Hz, $^5J(H,H) = 0.7$ Hz, 2H; H-6), 7.88 (ddd, $^3J(H,H) = 7.7$, 4.8 Hz, $^4J(H,H) = 1.1$ Hz, 2H; H-3), 7.69 (dddd, $^3J(H,H) = 7.7$, 7.4 Hz, $^4J(H,H) \approx {}^4J(P,H) \approx 2.0$ Hz, 2H; H-4), 7.43 (ddd, $^3J(H,H) = 8.5$, 7.1 Hz, $^4J(H,H) = 1.9$ Hz, 2H; H-8), 7.23 (ddd, $^3J(H,H) =$ 7.4, $^3J(P,H) = 4.8$ Hz, $^4J(H,H) = 1.1$ Hz, 2H; H-5), 6.81 (d, $^3J(H,H) =$ 8.5 Hz, 2H; H-9), 6.57 (ddd, $^3J(H,H) = 7.1$, 4.9 Hz, $^4J(H,H) = 0.7$ Hz, 2H; H-7), 5.10 (dd, $^2J(H,H) = 14.7$ Hz, $^2J(P,H) = 7.3$ Hz, 4H; H-1_{eq}), 4.08 ppm (dd, $^2J(H,H) = 14.7$ Hz, $^2J(P,H) = 4.4$ Hz, 4H; H-1_{ax}); $^{31}P\{^1H\}$ NMR (162 MHz, $CDCl_3$): $\delta = -33.5$ ppm; elemental analysis calcd (%) for $C_{24}H_{24}N_6P_2$: C 62.88, H 5.28, N 18.33, P 13.51; found: C 62.82, H 5.26, N 18.27, P 13.76.

Compound 4: Compound **2** (2.14 g, 12.5 mmol) was dissolved in dry ethanol (10 mL) and a solution of *m*-toluidine (1.35 g, 12.6 mmol) in dry ethanol (7 mL) was added. The mixture was stirred at 70 °C for 6 h, then at rt overnight. The precipitate formed was filtered off, washed carefully with ethanol, and dried at 0.05 torr for 3 h to give **4** (2.3 g, 75%). Single crystals of **4** suitable for X-ray crystal structure analysis were obtained by slow evaporation of $CDCl_3$ from an NMR sample. M.p. 161–165 °C; ^{1}H NMR (400 MHz, $CDCl_3$): $\delta = 8.75$ (brd, $^3J(H,H) = 4.4$ Hz, 2H; H-2), 7.73–7.63 (m, 4H; H-3+H-4), 7.23–7.25 (m, 2H; H-5), 7.11 (dd, $^3J(H,H) = 8.3$, 7.8 Hz, 2H; H-9), 6.68 (dd, $^3J(H,H) = 8.3$ Hz, $^4J(H,H) = 2.4$ Hz, 2H; H-10), 6.64 (brs, 2H; H-7), 6.54 (d, $^3J(H,H) = 7.8$ Hz, 2H; H-8), 4.59 (dd, $^2J(H,H) \approx {}^2J(P,H) \approx 14.7$ Hz, 4H; H-1_{eq}), 4.14 (dd, $^2J(H,H) = 14.7$ Hz, $^2J(P,H) = 4.4$ Hz, 4H; H-1_{ax}), 2.27 ppm (s, 6H; H-6); ^{13}C NMR (101 MHz, $CDCl_3$): $\delta = 162.6$ (m, $^1J(C,P) = 11.1$ Hz; *ipso*-C–P), 150.53 (dddd, $^1J(C,H) = 178.6$ Hz, $^2J(C,H) = 6.6$ Hz, $^3J(C,P) \approx {}^3J(C,H) = 3.3$ Hz; C-2), 146.07 (m; *ipso*-C–N), 138.82–138.51 (m; *ipso*-C–C), 135.59 (ddd, $^1J(C,H) = 162.9$ Hz, $^2J(C,H) = 6.6$, 7.5 Hz; C-4), 129.02 (ddd, $^1J(C,H) = 163.6$ Hz, $^2J(C,H) = 6.6$ Hz, $^2J(C,P) = 33.7$ Hz; C-5), 128.98 (d, $^1J(C,H) = 157.1$ Hz; C-7), 122.73 (ddd, $^1J(C,H) = 164.3$ Hz, $^2J(C,H) = 7.5$, 6.6 Hz; C-3), 117.85 (ddd, $^1J(C,H) = 158.6$ Hz, $^2J(C,H) = 11.6$ Hz, $^3J(C,H) = 6.4$ Hz; C-8) 113.75 (brd, $^1J(C,H) = 155.5$ Hz; C-9), 110.17 (d, $^1J(C,H) = 157.1$ Hz; C-10), 56.45 (tdd, $^1J(C,H) = 140.8$ Hz, $^1J(C,P) =$ 16.5 Hz, $^3J(C,P) = 4.6$ Hz; C-1), 22.08 ppm (qdd, $^1J(C,H) = 126.1$ Hz, $^3J(C,H) \approx {}^3J(C,H) = 4.6$ Hz; C-6); $^{31}P\{^1H\}$ NMR (162 MHz, $CDCl_3$): $\delta =$ −43.4 ppm; elemental analysis calcd (%) for $C_{28}H_{30}N_4P_2$: C 69.41, H 6.24, N 11.56, P 12.79; found: C 69.43, H 6.26, N 11.62, P 12.76.

Compound 5: Compound **5** (1.12 g, 85%) was prepared by the procedure described above for **4** from **2** (0.92 g, 5.4 mmol) and *p*-toluidine (0.58 g, 5.4 mmol), except the reaction mixture was stirred at ambient temperature for 30 min. Single crystals of **5** suitable for X-ray crystal structure analysis were obtained by recrystallisation of crude **5** from toluene. M.p. 170 °C; ^{1}H NMR (400 MHz, $CDCl_3$): $\delta = 8.73$ (brd, $^3J(H,H) = 4.7$ Hz, 2H; H-2), 7.69–7.65 (m, 4H; H-3+H-4), 7.24–7.21 (m, 2H; H-5), 7.01 (d, $^3J(H,H) = 7.8$ Hz, 4H; H-8), 6.76 (d, $^3J(H,H) = 7.8$ Hz, 4H; H-7), 4.60 (dd, $^2J(H,H) = 15.0$ Hz, $^2J(P,H) \sim 12.5$ Hz, 4H; H-1_{eq}), 4.12 (dd, $^2J(H,H) = 15.0$ Hz, $^2J(P,H) =$ 4.8 Hz, 4H; H-1_{ax}), 2.20 ppm (s, 6H, H-6); $^{31}P\{^1H\}$ NMR (162 MHz, $CDCl_3$): $\delta = -44.2$ ppm; MS (EI): *m/z* (%): 484 (1.3) $[M]^+$, 406 (0.67) $[M-C_5H_4N]^+$, 374 (4.22) $[M-C_5H_5NP]^+$, 350 (10.68) $[M-C_7H_5NP]^+$, 255 (7.32) $[M-C_{13}H_{14}N_2P]^+$, 122 (46.84) $[C_6H_5NP]^+$, 91 (100.0) $[C_7H_7]^+$; elemental analysis calcd (%) for $C_{28}H_{30}N_4P_2$: C 69.41, H 6.24, N 11.56, P 12.79; found: C 69.54, H 6.26, N 11.47, P 12.76.

Compounds 6a and 6b: Compound **6a** (1.70 g, 63%) was prepared by the procedure described above for **4** from **2** (1.45 g, 8.47 mmol) and diphenylmethylamine (1.55 g, 8.47 mmol), except that the reaction time was 15 min. M.p. 194–196 °C; ^{1}H NMR (400 MHz, $CDCl_3$): $\delta = 8.16$ (brd, $^3J(H,H) = 4.4$ Hz, 2H; H-2), 7.60 (brd, $^3J(H,H) = 7.3$ Hz, 8H; H-7), 7.21 (dd, $^3J(H,H) = 7.3$, 7.9 Hz, 8H; H-8), 7.16–7.09 (m, $^3J(H,H) = 7.9$ Hz, 6H; H-9+H-4), 6.80 (dd, $^3J(H,H) = 6.9$, 4.9 Hz, 2H; H-3), 6.30 (d, $^3J(H,H) = 7.8$ Hz, 2H; H-5), 5.71 (s, 2H; H-6), 3.94 (brd, $^2J(H,H) = 14.7$ Hz, 4H; H-1_A), 3.64 ppm (brd, $^2J(H,H) = 14.7$ Hz, 4H; H-1_B); $^{31}P\{^1H\}$ NMR (162 MHz, $CDCl_3$): $\delta = -60.5$ ppm; elemental analysis calcd (%) for $C_{40}H_{38}N_4P_2$: C 75.46, H 6.02, N 8.80, P 9.73; found: C 75.38, H 6.16, N 8.87, P 9.76.

Crystals of **6b** (0.36 g, 8%) precipitated from the filtrate of the reaction mixture. They were filtered off, washed with ethanol, and dried at 0.05 torr for 2 h. M.p. 170–171 °C; ^{1}H NMR (400 MHz, $CDCl_3$): $\delta = 8.58$ (brd, $^3J(H,H) = 4.4$ Hz, 1H; H-2), 7.57 (dd, $^3J(H,H) =$ 7.3, 7.9 Hz, 1H; H-4), 7.44 (brd, $^3J(H,H) = 7.3$ Hz, 1H; H-3), 7.33–7.31 (m, 4H; H-9), 7.26–7.08 (m, 17H; H-7+H-8+H-5), 4.78 (s, 2H; H-6), 3.46 (dd, $^2J(H,H) = 11.3$ Hz, $^4J(H,H) = 2.0$ Hz, 1H; H-10_A), 3.40 (d, $^2J(H,H) = 11.3$ Hz, 1H; H-10_B), 3.30 (dd, $^2J(H,H) \approx {}^2J(P,H) \approx 13.2$ MHz, 2H; H-1_{eq}), 3.18 ppm (dd, $^2J(H,H) = 13.2$ Hz, $^2J(P,H) = 4.9$ Hz, 2H; H-1_{ax}); $^{31}P\{^1H\}$ NMR (162 MHz, $CDCl_3$): $\delta = -58.0$ ppm; elemental analysis calcd (%) for $C_{34}H_{32}N_3P$: C 79.51, H 6.28, N 8.18, P 6.03; found: C 79.38, H 6.26, N 8.27, P 6.06.

Compound 7a: Compound **7a** (1.51 g, 60%) was prepared by the procedure described above for **4** from **2** (1.78 g, 10.4 mmol) and benzylamine (1.13 g, 10.6 mmol), except that the reaction mixture was stirred at 60 °C for 3 h. An analytically pure sample of **7a** was obtained by recrystallization from toluene. Single crystals of **7a** suitable for X-ray crystal structure analysis were obtained by recrys-

tallization from toluene. M.p. 170 °C; ^{1}H NMR (400 MHz, [D$_6$]DMSO): δ = 8.49 (br d, ^3J(H,H) = 4.4 Hz, 2H; H-2), 7.56 (dd, ^3J(H,H) = 7.3, 7.8 Hz, 2H; H-4), 7.38 (br d, ^3J(H,H) = 7.3 Hz, 4H; *m*-Bn), 7.28–7.32 (m, ^3J(H,H) = 7.3, Hz, 6H, *o*-+*p*-Bn), 7.19 (br d, ^3J(H,H) = 7.8 Hz, 2H; H-5), 7.14 (dd, ^3J(H,H) = 7.3, 4.4 Hz, 2H; H-3), 4.17 (s, 4H; H-6), 3.73 ppm (br s, 8H; H-1); ^{31}P{^{1}H} NMR (162 MHz, [D$_6$]DMSO): δ = −60.3 ppm; elemental analysis calcd (%) for $C_{28}H_{30}N_4P_2$: C 69.41, H 6.24, N 11.56, P 12.79; found: C 69.78, H 6.26, N 11.37, P 12.96.

Compounds 8a and 8b: Compound **8a** (0.99 g, 50%) was prepared by the procedure described above for **4** from **2** (1.32 g, 7.7 mmol) and (*R*)-α-methylbenzylamine (0.93 g, 7.7 mmol), except that the reaction time was 2 h. M.p. 132–133 °C; $[\alpha]_D^{20}$ = −15 cm^3 g^{-1} dm^{-1} (*c* = 0.17 in C_6H_6); ^{1}H NMR (400 MHz, $CDCl_3$): δ = 8.50 (br d, ^3J(H,H) = 4.6 Hz, 2H; H-2), 7.49 (br d, ^3J(H,H) = 7.3 Hz, 4H; *m*-PhCH), 7.32–7.29 (m, ^3J(H,H) = 7.3, 7.4 Hz, 6H; *o*-+*p*-PhCH), 7.22 (dd, ^3J(H,H) ≈ ^3J(H,H) ≈ 7.3 Hz, 2H; H-4), 6.97 (dd, ^3J(H,H) = 7.3, 4.6 Hz, 2H; H-3), 6.75 (d, ^3J(H,H) = 7.3 Hz, 2H; H-5), 4.73 (q, ^3J(H,H) = 6.6 Hz, 2H; H-6), 4.58 (br d, ^3J(H,H) = 14.8 Hz, 2H; H-1$_A$), 3.63 (br d, ^3J(H,H) = 14.8 Hz, 2H; H-1$_B$), 3.57 (br d, ^3J(H,H) = 14.6 Hz, 2H; H-1$_{A'}$), 3.46 (br d, ^3J(H,H) = 14.6 Hz, 2H; H-1$_{B'}$), 1.49 ppm (d, ^3J(H,H) = 6.6 Hz, 6H; H-7); ^{31}P{^{1}H} NMR (162 MHz, $CDCl_3$): δ = −63.1 ppm; MS (EI): *m/z* (%): 512 (0.06) $[M]^+$, 434 (0.25) $[M-C_5H_4N]^+$, 407 (0.25) $[M-C_6H_5(CH)CH_3]^+$, 402 (4.13) $[M-C_5H_5NP]^+$, 364 (3.15) $[M-C_{10}H_{14}N]^+$, 256 (7.83) $[C_{15}H_{17}N_2P]^+$, 151 (19.49) $[C_5H_5NP(CH)CH_2N]^+$, 124 (13.79) $[C_6H_7NP]^+$, 105 (100.0) $[C_8H_9]^+$; elemental analysis calcd (%) for $C_{30}H_{34}N_4P_2$: C 70.30, H 6.69, N 10.93, P 12.09; found: C 70.38, H 6.56, N 11.03, P 12.06.

Crystals of **8b** (0.09 g, 3%) precipitated from the filtrate of the reaction mixture. They were filtered off, washed with ethanol, and dried at 0.05 torr for 2 h. M.p. 92–94 °C; $[\alpha]_D^{20}$ = +35 cm^3 g^{-1} dm^{-1} (*c* = 0.17 in $CHCl_3$); ^{1}H NMR (400 MHz, $CDCl_3$): δ = 8.58 (br d, ^3J(H,H) = 4.2 Hz, 1H; H-2), 7.51 (dd, ^3J(H,H) = 8.2, 7.6 Hz, 1H; H-4), 7.18–7.30 (m, 11H; Ph+H-5), 7.10 (dd, ^3J(H,H) = 8.2, 4.2 Hz, 1H; H-3), 3.98 (q, ^3J(H,H) = 6.7 Hz, 1H; H-6), 3.84 (q, ^3J(H,H) = 6.5 Hz, 1H; H-6′), 3.62–3.45 (m, 4H; H-10+H-1$_A$), 3.30–3.28 (m, 2H; H-1$_B$), 1.37 (d, ^3J(H,H) = 6.5 Hz, 3H; H-7′), 1.19 ppm (d, ^3J(H,H) = 6.7 Hz, 2H; H-7); ^{31}P{^{1}H} NMR (162 MHz, $CDCl_3$): δ = −58.1 ppm; elemental analysis calcd (%) for $C_{24}H_{28}N_3P$: C 74.01, H 7.25, N 10.79, P 7.95; found: C 73.88, H 7.16, N 10.75, P 7.89.

Compound 9: A solution of [$PtCl_2$(cod)] (0.062 g, 0.17 mmol) in CH_2Cl_2 (5 mL) was added to a stirred solution of **7a** (0.08 g, 0.17 mmol) in CH_2Cl_2 (5 mL). The mixture was stirred for 30 min. CH_2Cl_2 was removed under reduced pressure to give a light-yellow solid, then Et_2O (5 mL) was added. The solid was filtered off and dried under reduced pressure to give **9** (0.08 g, 62%). M.p. > 260 °C; ^{1}H NMR (400 MHz, $CDCl_3$): δ = 8.61 (br d, ^3J(H,H) = 4.5 Hz, 2H; H-2), 7.98–7.93 (m, 2H; H-4), 7.78–7.72 (m, 2H; H-3), 7.43 (d, ^3J(H,H) = 7.0 Hz, 4H; H-8), 7.38–7.31 (m, ^3J(H,H) = 7.0 Hz, 8H; H-7+H-9+H-3), 4.40 (s, 4H; H-6), 3.86 (dd, ^2J(H,H) = 14.0 Hz, ^2J(P,H) = 5.8 Hz, 4H; H-1$_A$), 3.78 ppm (dd, ^2J(H,H) = 14.0 Hz, ^2J(P,H) = 5.1 Hz, 4H, H-1$_B$); ^{31}P{^{1}H} NMR (162 MHz, $CDCl_3$): δ = −24.2 (^1J(Pt,P) = 2910 Hz); IR (nujol): $\tilde{\nu}$ = 288, 315 cm^{-1} (PtCl); elemental analysis calcd (%) for $C_{28}H_{30}Cl_2N_4P_2Pt$: C 44.81, H 4.03, Cl 9.45, N 7.47, P 8.25; found: C 44.78, H 3.96, Cl 9.24, N 7.23, P 8.36.

Compound 10: Compound **10** was prepared by the procedure described above for **9** from **5** (0.10 g, 0.21 mmol) and [$PtCl_2$(cod)] (0.077 g, 0.21 mmol), except that the reaction time was 2 d and the reaction mixture was yellow. CH_2Cl_2 was removed under reduced pressure to give a light-yellow solid, to which Et_2O (5 mL) was added. The solid was filtered off, carefully washed with cold $CHCl_3$, and dried under reduced pressure to give **10** (0.10 g, 65%). Single crystals of **10** suitable for X-ray crystal-structure analysis were obtained by slow diffusion of *n*-hexane into a solution of **10** in CH_2Cl_2. M.p. 260 °C; ^{1}H NMR (400 MHz, $CDCl_3$): δ = 8.76 (br s, 2H; H-2), 8.24 (m, 2H; H-4), 7.82 (m, 2H; H-3), 7.41 (m, 2H; H-5), 7.13 (d, ^3J(H,H) = 7.8 Hz, 4H; H-8), 6.99 (d, ^3J(H,H) = 7.8 Hz, 4H; H-7), 4.66 (d, ^2J(H,H) = 14.4 Hz, 4H; H-1$_A$), 4.22 (dd, ^2J(H,H) = 14.4 Hz, ^2J(P,H) = 6.4 Hz, 4H; H-1$_B$), 2.27 ppm (s, 6H; H-6); ^{31}P{^{1}H} NMR (162 MHz, $CDCl_3$): δ = −12.5 ppm (^1J(Pt,P) = 3054 Hz); IR (nujol): $\tilde{\nu}$ = 290, 317 cm^{-1} (PtCl); elemental analysis calcd (%) for $C_{28}H_{30}Cl_2N_4P_2Pt$: C 44.81, H 4.03, Cl 9.45, N 7.47, P 8.25; found: C 44.68, H 4.06, Cl 9.46, N 7.51, P 8.19.

Compound 11: Compound **11** (0.14 g, 92%) was prepared by the procedure described above for **10** from **5** (0.11 g, 0.23 mmol) and [$PdCl_2$(cod)] (0.065 g, 0.23 mmol), except that the reaction time was 1 d, the reaction mixture was red, and the resultant red solid was washed with diethyl ether. Single crystals of **11** suitable for X-ray crystal-structure analysis were obtained by slow diffusion of *n*-hexane into a solution of **11** in CH_2Cl_2. M.p. 258 °C; ^{1}H NMR (400 MHz, $CDCl_3$): δ = 8.75 (d, ^3J(H,H) = 4.6 Hz, 2H; H-2), 8.23 (d, ^3J(H,H) = 7.8, 4.6 Hz, 2H; H-3), 7.80 (ddd, ^3J(H,H) = 7.8, 10.8 Hz, ^4J(H,H) = 1.6 Hz, 2H; H-4), 7.41 (m, 2H; H-5), 7.15 (d, ^3J(H,H) = 8.2 Hz, 4H; H-8), 7.00 (d, ^3J(H,H) = 8.2 Hz, 4H; H-7), 4.72 (d, ^2J(H,H) = 14.0 Hz, 4H; H-1$_A$), 4.06 (dd, ^2J(H,H) = 14.0 Hz, ^2J(P,H) = 3.7 Hz, 4H; H-1$_B$), 2.28 ppm (s, 6H; H-6); ^{31}P{^{1}H} NMR (162 MHz, $CDCl_3$): δ = 3.5 ppm; IR (Nujol): $\tilde{\nu}$ = 296, 282 cm^{-1} (PdCl); elemental analysis calcd (%) for $C_{28}H_{30}Cl_2N_4P_2Pd$: C 50.81, H 4.57, Cl 10.71, N 8.47, P 9.36; found: C 50.68, H 4.46, Cl 10.66, N 8.51, P 9.49.

Compound 12: A solution of [$PtCl_2$(cod)] (0.047 g, 0.13 mmol) in CH_2Cl_2 (5 mL) was added to a stirred solution of **5** (0.12 g, 0.25 mmol) in CH_2Cl_2 (5 mL). The yellow mixture was stirred for 30 min. CH_2Cl_2 was removed under reduced pressure to give a light-yellow solid, to which Et_2O (5 mL) was added. The solid was filtered off, washed with diethyl ether, and dried under reduced pressure to give **12** (0.10 g, 62%). Single crystals of **12** suitable for X-ray crystal-structure analysis were obtained by slow evaporation of a solution of **12** in $CDCl_3$. M.p. 200 °C; ^{1}H NMR (400 MHz, CD_2Cl_2): δ = 8.34 (d, ^3J(H,H) = 3.8 Hz, 2H; H-2), 7.58 (d, ^3J(H,H) = 7.2 Hz, 2H; H-5), 7.48 (dd, ^3J(H,H) = 7.2, 7.0 Hz, 2H; H-4), 7.16 (dd, ^3J(H,H) = 7.0, 3.8 Hz, 2H; H-3), 7.07 (d, ^3J(H,H) = 8.1 Hz, 4H; H-8), 6.94 (d, ^3J(H,H) = 8.1 Hz, 4H; H-7), 4.75 (d, ^2J(H,H) = 13.9 Hz, 4H; H-1$_A$), 4.15 (d, ^2J(H,H) = 13.9 Hz, ^3J(Pt,H) = 42.2 Hz, 4H; H-1$_B$), 2.14 ppm (s, 6H; H-6); ^{1}H NMR (400 MHz, D_2O): δ = 8.55 (d, ^3J(H,H) = 4.6 Hz, 2H; H-2), 7.61 (dd, ^3J(H,H) ≈ ^3J(H,H) ≈ 7.2 Hz, 2H; H-4), 7.44–7.39 (m, ^3J(H,H) = 8.2 Hz, 6H; H-3+H-8), 7.34 (d, ^3J(H,H) = 8.2 Hz, 4H; H-7), 6.89 (d, ^3J(H,H) = 7.2 Hz, 2H; H-5), 4.29 (s, ^3J(Pt,H) = 31.9 Hz, 8H; H-1), 2.30 ppm (s, 6H; H-6); ^{1}H NMR (400 MHz, $CDCl_3$): δ = 8.43 (d, ^3J(H,H) = 4.3 Hz, 2H; H-2), 7.67–7.60 (m, 4H; H-5+H-4), 7.28–7.25 (m, 2H; H-3, the signal partially overlaps with the solvent signal), 7.17 (d, ^3J(H,H) = 8.2 Hz, 4H; H-8), 7.03 (d, ^3J(H,H) = 8.2 Hz, 4H; H-7), 4.79 (d, ^2J(H,H) = 13.9 Hz, 4H; H-1$_A$), 4.25 (d, ^2J(H,H) = 13.9 Hz, ^3J(Pt,H) = 42.2 Hz, 4H; H-1$_B$), 2.21 ppm (s, 6H; H-6); ^{31}P{^{1}H} NMR (162 MHz, CD_2Cl_2): δ = −15.4 ppm (^1J(Pt,P) = 2274.2); ^{31}P{^{1}H} NMR (162 MHz, $CDCl_3$): δ = −14.3 ppm (^1J(Pt,P) = 2241.7 Hz); ^{31}P{^{1}H} NMR (162 MHz, D_2O): δ = −14.8 ppm (^1J(Pt,P) = 2082.4 Hz); elemental analysis calcd (%) for $C_{56}H_{60}Cl_2N_8P_4Pt$: C 54.46, H 4.90, Cl 5.74, N 9.07, P 10.03; found: C 54.68, H 4.86, Cl 5.56, N 9.11, P 9.99.

Compound 13: Compound **13** (0.06 g, 55%) was prepared as described above for **12** from **5** (0.10 g, 0.21 mmol) and [$PdCl_2$(cod)] (0.029 g, 0.10 mmol), except that the reaction mixture was red. Single crystals of **13** suitable for X-ray crystal-structure analysis were obtained by slow evaporation of a solution of **13** in $CDCl_3$. M.p. > 260 °C; ^{1}H NMR (400 MHz, $CDCl_3$): δ = 8.38 (d, ^3J(H,H) = 4.2 Hz, 2H; H-2), 7.70 (d, ^3J(H,H) = 7.5 Hz, 2H; H-5), 7.58 (dd, ^{3}J(H,H) = 7.2, 7.5 Hz, 2H; H-4), 7.29 (dd, ^3J(H,H) = 7.2, 4.2 Hz, 2H; H-3), 7.06 (d, ^3J(H,H) = 8.1 Hz, 4H; H-8), 6.96 (d, ^3J(H,H) = 8.1 Hz, 4H;

H-7), 4.82 (d, ^2J(H,H) = 13.8 Hz, 4H; H-1$_A$), 3.96 (d, ^2J(H,H) = 13.8 Hz, 4H; H-1$_B$), 2.21 ppm (s, 6H; H-6); ^{1}H NMR (400 MHz, D_2O): δ = 8.62 (d, ^3J(H,H) = 4.4 Hz, 2H; H-2), 7.64 (dd, ^3J(H,H) = 8.1, 7.2 MHz, 2H; H-4), 7.46 (d, ^3J(H,H) = 8.4 Hz, 4H; H-8), 7.42 (dd, ^3J(H,H) = 7.2, 4.4 Hz, 2H; H-5), 7.37 (d, ^3J(H,H) = 8.4 Hz, 4H; H-7), 7.09 (d, ^3J(H,H) = 8.1 Hz, 2H; H-5), 4.37 (br d, ^2J(H,H) = 14.0 Hz, 4H; H-1$_A$), 4.14 (d, ^2J(H,H) = 14.0 Hz, 4H; H-1$_B$), 2.34 ppm (s, 6H; H-6); ^{31}P{^{1}H} NMR (162 MHz, $CDCl_3$): δ = −0.6 ppm; ^{31}P{^{1}H} NMR (D_2O): δ = −9.8 ppm; MS (MALDI): *m/z*: 1074 $[M-2Cl]^+$; elemental analysis calcd (%) for $C_{56}H_{60}Cl_2N_8P_4Pd$: C 58.67, H 5.28, Cl 6.19, N 9.77, P 10.81; found: C 58.81, H 5.24, Cl 6.25, N 9.69, P 10.76.

Compound 14: Compound **14** (0.11 g, 92%) was prepared by the procedure described above for **12** from **8a** (0.10 g, 0.19 mmol) and $[PtCl_2(cod)]$ (0.028 g, 0.09 mmol), except that the reaction time was 1 d and the reaction mixture was dark red. M.p. 140–142 °C; $[\alpha]_D^{20}$ = +9 cm^3 g^{-1} dm^{-1} (*c* = 0.03 in CH_2Cl_2); ^{1}H NMR (400 MHz, $CDCl_3$): δ = 8.14 (d, ^3J(H,H) = 3.6 Hz, 2H; H-2), 7.68 (d, ^3J(H,H) = 7.2 Hz, 2H; H-5), 7.43 (dd, ^3J(H,H) = 7.2, 7.6 Hz, 2H; H-4), 7.22–7.31 (m, 10H; Ph), 7.07 (dd, ^3J(H,H) = 7.6, 3.6 Hz, 2H; H-3), 4.28 (q, ^3J(H,H) = 6.4 Hz, 2H; H-7), 4.18 (d, ^2J(H,H) = 13.1 Hz, 2H; H-1$_A$), 4.11 (d, ^2J(H,H) = 11.9 Hz, 2H; H-1$_{A'}$), 3.62 (d, ^2J(H,H) = 11.9 Hz, 2H; H-1$_{B'}$), 3.56 (d, ^2J(H,H) = 13.1 Hz, 2H; H-1$_B$), 1.56 ppm (d, ^3J(H,H) = 6.4 Hz, 3H; H-6); ^{1}H NMR (400 MHz, D_2O): δ = 8.34 (d, ^3J(H,H) = 4.0 Hz, 2H; H-2), 7.48 (dd, ^3J(H,H) = 8.2, 7.3 Hz, 2H; H-4), 7.42–7.37 (m, 10H; Ph), 7.27 (dd, ^3J(H,H) = 4.0, 8.2 Hz, 2H; H-3), 7.01 (d, ^3J(H,H) = 7.3 Hz, 2H; H-5), 4.31 (q, ^3J(H,H) = 6.4 Hz, 2H; H-7), 4.09 (d, ^2J(H,H) = 14.5 Hz, 2H; H-1$_A$), 4.00 (d, ^2J(H,H) = 14.5 Hz, 2H; H-1$_B$), 3.86 (d, ^2J(H,H) = 13.9 Hz, 2H; H-1$_{A'}$), 3.47 (d, ^2J(H,H) = 13.9 Hz, 2H; H-1$_{B'}$), 1.59 ppm (d, ^3J(H,H) = 6.4 Hz, 3H; H-6); ^{31}P{^{1}H} NMR (162 MHz, $CDCl_3$): δ = −11.7 ppm (^1J(PtP) = 2258.5 Hz); ^{31}P{^{1}H} NMR (D_2O): δ = −10.8 ppm (^1J(PtP) = 2096 Hz); elemental analysis calcd (%) for $C_{60}H_{68}Cl_2N_8P_4Pt$: C 55.82, H 5.31, Cl 5.49, N 8.68, P 9.60; found: C 55.75, H 5.36, Cl 5.54, N 8.49, P 9.69.

Compound 15: A solution of $[NiBr_2(dme)]$ (0.049 g, 0.16 mmol) in CH_2Cl_2 (5 mL) was added dropwise to a stirred solution of **5** (0.163 g, 0.33 mmol) in CH_2Cl_2 (7 mL). The dark-red reaction mixture was stirred for 1 d. CH_2Cl_2 was removed under reduced pressure to give a solid, then Et_2O (5 mL) was added. The solid was filtered off, washed with diethyl ether, and dried under reduced pressure to give **15** (0.12 g, 63%). M.p. 230–231 °C; ^{1}H NMR (400 MHz, $CDCl_3$): δ = 8.31 (m, 2H; H-2), 7.64 (m, 2H; H-3 or H-4 or H-5), 7.32 (m, 2H; H-3 or H-4 or H-5), 7.04 (m, 10H; H-3 or H-4 or H-5 + H-7 + H-8), 4.60 (m, 4H; H-1$_A$), 3.70 (m, 4H; H-1$_B$), 2.28 ppm (s, 6H; H-6); ^{1}H NMR (400 MHz, CD_3CN): δ = 8.28 (d, ^3J(H,H) = 3.6 Hz, 2H; H-2), 7.53–7.41 (m, 2H; H-4), 7.23 (dd, ^3J(H,H) = 3.6, 7.5 Hz, 2H; H-3), 7.06–6.96 (m, 10H; H-7+H-8+H-5), 4.54 (d, ^2J(H,H) = 13.5 Hz, 4H; H-1$_A$), 3.70 (br d, ^2J(H,H) = 13.5 Hz, 4H; H-1$_B$), 2.22 ppm (s, 6H; H-6); ^{31}P{^{1}H} NMR (162 MHz, $CDCl_3$): δ = 22.9 (br m), −10.6 ppm (br m); ^{31}P{^{1}H} NMR (162 MHz, CD_3CN): δ = 35.9 (br m), −11.4 ppm (br m); MS (MALDI): *m/z*: 1107 $[M-Br]^+$; elemental analysis calcd (%) for $C_{56}H_{60}Br_2N_8NiP_4$: C 56.64, H 5.09, Br 13.46, N 9.44, P 10.43; found: C 56.81, H 5.12, Br 13.25, N 9.62, P 10.32.

Compound 16: A solution of $[Ni(CH_3CN)_6][BF_4]_2$ (0.047 g, 0.21 mmol) in CH_3CN (5 mL) was added dropwise to a stirred suspension of **5** (0.101 g, 0.21 mmol) in CH_3CN (5 mL) The dark-red reaction mixture was stirred for 1 d. CH_3CN was removed under reduced pressure to give a solid. The solid was filtered off, washed with diethyl ether, and dried under reduced pressure to give **16** (0.23 g, 90%). Single crystals of **16** suitable for X-ray crystal structure analysis were obtained by slow diffusion of ethanol into a solution of **16** in acetone. M.p. 196–198 °C; ^{1}H NMR (400 MHz, CD_3CN): δ = 8.45 (d, ^3J(H,H) = 4.0 Hz, 2H; H-2), 7.52 (dd, ^3J(H,H) = 7.0, 7.4 Hz, 2H; H-4), 7.33 (dd, ^3J(H,H) = 7.0, 4.0 Hz, 2H; H-3), 7.21 (br s, 8H; H-7+H-8), 7.06 (br d, ^3J(H,H) = 7.4 Hz, 2H; H-5), 4.42 (d, ^2J(H,H) = 13.8 Hz, 4H; H-1$_A$), 3.97 (d, ^2J(H,H) = 13.8 Hz, 4H; H-1$_B$), 2.29 ppm (s, 6H; H-6); ^{31}P{^{1}H} NMR (162 MHz, CD_3CN): δ = 0.7 ppm; MS (MALDI): *m/z*: 1027 $[M-(BF_4)_2]^+$; elemental analysis calcd (%) for $C_{56}H_{60}B_2F_8N_8NiP_4$: C 55.99, H 5.03, N 9.33, P 10.31; found: C 55.12, H 5.12, N 9.61, P 10.23..

Compound 17: A solution of $[Ni(CH_3CN)_6][BF_4]_2$ (0.054 g, 0.14 mmol) in CH_3CN (3 mL) was added to a stirred solution of **8a** (0.14 g, 0.27 mmol) in a mixture of CH_3CN (3 mL) and CH_2Cl_2 (2 mL). The mixture was stirred for 1 d. The solvent was removed under reduced pressure to give **17** (0.17 g, 98%) as a red-violet solid. M.p. 158–160 °C; $[\alpha]_D^{20}$ = +10 cm^3 g^{-1} dm^{-1} (*c* = 0.17 in CH_3CN); ^{1}H NMR (400 MHz, $CDCl_3$): δ = 8.35 (d, ^3J(H,H) = 4.2 Hz, 2H; H-2), 7.43 (dd, ^3J(H,H) = 7.2, 7.6 Hz, 2H; H-4), 7.34–7.32 (m, 6H; Ph), 7.24 (dd, ^3J(H,H) = 7.6, 4.2 Hz, 2H; H-3 partiallly overlaps with phenyl group signals), 7.23–7.20 (m, 4H; Ph), 7.03 (d, ^3J(H,H) = 7.2 Hz, 2H; H-5), 4.06 (q, ^3J(H,H) = 6.9 Hz, 2H; H-6), 3.56 (br d, ^2J(H,H) = 13.1 Hz, 2H; H-1$_A$), 3.48 (br d, ^2J(H,H) = 13.2 Hz, 2H; H-1$_{A'}$), 3.08 (d, ^2J(H,H) = 13.1 Hz, 2H; H-1$_{B'}$), 2.99 (d, ^2J(H,H) = 13.1 Hz, 2H; H-1$_B$), 1.46 ppm (d, ^3J(H,H) = 6.9 Hz, 6H; H-7); ^{31}P{^{1}H} NMR (162 MHz, CD_3CN): δ = 5.4 ppm; MS (MALDI): *m/z*: 1083 $[M-(BF_4)_2]^+$; elemental analysis calcd (%) for $C_{60}H_{68}B_2F_8N_8NiP_4$: C 57.31, H 5.45, N 8.91, P 9.85; found: C 57.23, H 5.44, N 8.97, P 9.79.

Compound 18: A solution of ligand **5** (0.10 g, 0.21 mmol) in toluene (10 mL) was added to a stirred solution of $[W(CO)_4(cod)]$ (0.083 g, 0.21 mmol) in CH_2Cl_2 (5 mL). The reaction mixture was heated at 60 °C for 50 h. CH_2Cl_2 was removed under reduced pressure and Et_2O (5 mL) was added to the remaining solid. The brown solid was filtered off, washed with diethyl ether, and dried under reduced pressure to give **18** (0.12 g, 74%). Single crystals of **18** suitable for X-ray crystal structure analysis were obtained by slow diffusion of *n*-hexane into a solution of **18** in $CDCl_3$. M.p. > 260 °C; ^{1}H NMR (400 MHz, $CDCl_3$): δ = 8.71 (d, ^3J(H,H) = 5.1 Hz, 2H; H-2), 8.03 (m, 2H; H-3), 7.86 (dd, ^3J(H,H) ≈ ^3J(H,H) = 7.3 Hz, 2H; H-4), 7.33 (m, 2H; H-5), 7.05 (d, ^3J(H,H) = 7.9 Hz, 4H; H-8), 6.98 (d, ^3J(H,H) = 7.9 Hz, 4H; H-7), 4.38 (br d, ^2J(H,H) = 13.3 Hz, 4H; H-1$_A$), 3.91 (d, ^2J(H,H) = 13.3 Hz, 4H; H-1$_B$), 2.24 ppm (s, 6H; H-6); ^{31}P{^{1}H} NMR (162 MHz, $CDCl_3$): δ = 2.6 ppm (^1J(W,P) = 204 Hz); IR (nujol): $\tilde{\nu}$ = 2014, 1920, 1902, 1863 cm^{-1} (CO); elemental analysis calcd (%) for $C_{32}H_{30}N_4O_4P_2W$: C 49.25, H 3.87, N 7.18, P 7.94; found: C 49.34, H 3.85, N 7.11, P 7.79.

Compound 19: Solid $NiCl_2$ (0.05 g, 0.38 mmol) was added to a solution of 1,3,5,7-tetraphenyl-1,5-diaza-3,7-diphosphacyclooctane[32a, b] (0.35 g, 0.77 mmol) in DMF (20 mL) and the mixture was stirred for 24 h. The solvent was evaporated under reduced pressure, then the resultant dark-red powder was washed with ethanol (20 mL), and dried under reduced pressure to give **19** (0.31 g, 79%). Single crystals of **19** suitable for X-ray crystal-structure analysis were obtained by slow evaporation of a solution of **19** in chloroform. M.p. 179–183 °C; ^{1}H NMR (CD_3CN): δ = 7.76–6.87 (m, 20H; Ph), 4.67–4.43 (m, 4H; P–CH_2–N), 3.96–3.67 ppm (m, 4H; P–CH_2–N); ^{31}P{^{1}H} NMR (CD_3CN): δ = 21.6 (m), −14.0 ppm (m); MS (MALDI): *m/z*: 1003 $[M-Cl]^+$; elemental analysis calcd (%) for $C_{56}H_{56}Cl_2N_4NiP_4$: C 64.76, H 5.43, Cl 6.83, N 5.39, Ni 5.65, P 11.93; found: C 64.73, H 5.41, Cl 6.74, N 5.65, Ni 5.63, P 11.62.

Acknowledgements

Financial support from RFBR (No. 12-03-97083-r_povolzhye_a, 13-03-00139, 13-03-00563), President's of RF Grant for the support of leading scientific schools (No. NSh-4428.2014.3), the Ministry of Science and Education (state contract 8432) and

the VolkswagenStiftung, Germany (Az. 85 625) is gratefully acknowledged.

Keywords: diazadiphosphacyclooctanes · electrochemistry · hydrogen · metal complexes · pyridylphosphines

[1] P. Espinet, K. Soulantica, *Coord. Chem. Rev.* **1999**, *193 – 195*, 499 – 556.
[2] C.-M. Tanga, Y. Zenga, X.-G. Yanga, Y.-C. Leia, G.-Y. Wang, *J. Mol. Catal. A* **2009**, *314*, 15 – 20.
[3] H. Ishii, M. Goyal, M. Ueda, K. Takeuchi, M. Asai, *J. Mol. Catal. A* **1999**, *148*, 289 – 293.
[4] F. Speiser, P. Braunstein, L. Saussine, *Organometallics* **2004**, *23*, 2625 – 2632.
[5] F. Speiser, P. Braunstein, L. Saussine, *Organometallics* **2004**, *23*, 2633 – 2640.
[6] J. Flapper, H. Kooijman, M. Lutz, A. L. Spek, P. W. N. M. Van Leeuwen, C. J. Elsevier, P. C. J. Kamer, *Organometallics* **2009**, *28*, 1180 – 1192.
[7] C. Federsel, R. Jackstell, A. Boddien, G. Laurenczy, M. Beller, *ChemSusChem* **2010**, *3*, 1048 – 1050.
[8] P. Kumar, A. K. Singh, M. Yadav, P.-Z. Li, S. K. Singh, Q. Xu, D. S. Pandey, *Inorg. Chim. Acta* **2011**, *368*, 124 – 131.
[9] Z. Xue, B. W. Lee, S. K. Noh, W. S. Lyoo, *Polymer* **2007**, *48*, 4704 – 4714.
[10] D. He, Z. Xue, M. Y. Khan, S. K. Noh, W. S. Lyoo, *J. Polym. Sci. Part A* **2010**, *48*, 144 – 151.
[11] X. Tan, L. Li, J. Zhang, X. Han, L. Jiang, F. Li, C.-Y. Su, *Chem. Mater.* **2012**, *24*, 480 – 485.
[12] D. B. Grotjahn, *Chem. Eur. J.* **2005**, *11*, 7146 – 7153.
[13] M. Jiménez-Tenorio, M. Carmen Puerta, P. Valerga, S. Moncho, G. Ujaque, A. Lledos, *Inorg. Chem.* **2010**, *49*, 6035 – 6057.
[14] T. Oshiki, H. Yamashita, K. Sawada, M. Utsunomiya, K. Takahashi, K. Takai, *Organometallics* **2005**, *24*, 6287 – 6290.
[15] D. Grotjahn, D. Lev, *J. Am. Chem. Soc.* **2004**, *126*, 12232 – 12233.
[16] A. Labonne, T. Kribber, L. Hintermann, *Org. Lett.* **2006**, *8*, 5853 – 5856.
[17] A. A. Karasik, S. V. Bobrov, G. N. Nikonov, A. P. Pisarevskiy, I. A. Litvinov, A. S. Dokutshaev, Yu. T. Strutshkov, K. M. Enikeev, *Russ. J. Coord. Chem.* **1995**, *21*, 574 – 584.
[18] A. A. Karasik, G. N. Nikonov, A. S. Dokutshaev, I. A. Litvinov, *Russ. J. Coord. Chem.* **1994**, *20*, 300 – 303.
[19] A. A. Karasik, R. N. Naumov, A. S. Balueva, Yu. S. Spiridonova, O. N. Golodkov, H. V. Novikova, G. P. Belov, S. A. Katsyuba, E. E. Vandyukova, P. Lönnecke, E. Hey-Hawkins, O. G. Sinyashin, *Heteroat. Chem.* **2006**, *17*, 499 – 513.
[20] M. Rakowski DuBois, D. L. DuBois, *C. R. Chim.* **2008**, *11*, 805 – 817.
[21] M. Rakowski DuBois, D. L. Dubois, *Chem. Soc. Rev.* **2009**, *38*, 62 – 72.
[22] A. Fihri, D. Luart, C. Len, A. Solhy, C. Chevrin, V. Polshettiwar, *Dalton Trans.* **2011**, *40*, 3116 – 3121.
[23] a) U. J. Kilgore, J. A. S. Roberts, D. H. Pool, A. M. Appel, M. P. Stewart, M. Rakowski DuBois, W. G. Dougherty, W. S. Kassel, R. M. Bullock, D. L. Dubois, *J. Am. Chem. Soc.* **2011**, *133*, 5861 – 5872; b) A. D. Wilson, R. K. Shoemaker, A. Miedaner, J. T. Muckerman, D. L. DuBois, M. Rakowski DuBois, *Proc. Natl. Acad. Sci. USA* **2007**, *104*, 6951 – 6956; c) M. H. Helm, M. P. Stewart, R. M. Bullock, M. Rakowski DuBois, D. L. Dubois, *Science* **2011**, *333*, 863 – 866; d) S. Wiese, U. J. Kilgore, D. L. Dubois, R. M. Bullock, *ACS Catal.* **2012**, *2*, 720 – 727; e) M. P. Stewart, M.-H. Ho, S. Wiese, M. L. Lindstrom, C. E. Thogerson, S. Raugei, R. M. Bullock, M. L. Helm, *J. Am. Chem. Soc.* **2013**, *135*, 6033 – 6046; f) D. H. Pool, D. L. DuBois, *J. Organomet. Chem.* **2009**, *694*, 2858 – 2865.
[24] J. Y. Yang, S. Chen, W. G. Dougherty, W. S. Kassel, R. M. Bullock, D. L. DuBois, S. Raugei, R. Rousseau, M. Dupuis, M. Rakowski DuBois, *Chem. Commun.* **2010**, *46*, 8618 – 8620.
[25] J. Y. Yang, R. M. Bullock, W. G. Dougherty, W. S. Kassel, B. Twamley, D. L. DuBois, M. Rakowski DuBois, *Dalton Trans.* **2010**, *39*, 3001 – 3010.
[26] B. R. Galan, J. C. Linehan, A. M. Appel, J. A. S. Roberts, U. J. Kilgore, J. Y. Yang, D. L. Dubois, J. Schoeffel, C. Seu, C. P. Kubiak, M. L. Helm, *J. Am. Chem. Soc.* **2011**, *133*, 12767 – 12779.
[27] S. E. Smith, J. Y. Yang, D. L. DuBois, R. M. Bullock, *Angew. Chem.* **2012**, *124*, 3206 – 3209; *Angew. Chem. Int. Ed.* **2012**, *51*, 3152 – 3155.
[28] A. Le Goff, V. Artero, B. Jousselme, P. D. Tran, N. Guillet, R. Métayé, A. Fihri, S. Palacin, M. Fontecave, *Science* **2009**, *326*, 1384 – 1387.
[29] a) M. O'Hagan, W. J. Shaw, S. Raugei, Sh. Chen, J. Y. Yang, U. J. Kilgore, D. L. Dubois, R. M. Bullock, *J. Am. Chem. Soc.* **2011**, *133*, 14301 – 14312; b) M. O'Hagan, M.-H. Ho, J. Y. Yang, A. M. Appel, M. Rakowski DuBois, S. Raugei, W. J. Shaw, D. L. DuBois, R. M. Bullock, *J. Am. Chem. Soc.* **2012**, *134*, 19409 – 19424.
[30] a) U. J. Kilgore, M. P. Stewart, M. L. Helm, W. G. Dougherty, W. S. Kassel, M. Rakowski DuBois, D. L. DuBois, R. M. Bullock, *Inorg. Chem.* **2011**, *50*, 10908 – 10918; b) W. J. Shaw, M. L. Helm, D. L. DuBois, *Biochim. Biophys. Acta Bioenerg.* **2013**, *1827*, 1123 – 1139.
[31] a) A. A. Karasik, A. S. Balueva, O. G. Sinyashin, *C. R. Chim.* **2010**, *13*, 1151 – 1167; b) E. I. Musina, A. A. Karasik, A. S. Balueva, I. D. Strelnik, T. I. Fesenko, A. B. Dobrynin, T. P. Gerasimova, S. A. Katsyuba, O. N. Kataeva, P. Lönnecke, E. Hey-Hawkins, O. G. Sinyashin, *Eur. J. Inorg. Chem.* **2012**, 1857 – 1866; c) A. A. Karasik, A. A. Balueva, E. I. Moussina, R. N. Naumov, A. B. Dobrynin, D. B. Krivolapov, I. A. Litvinov, O. G. Sinyashin, *Heteroat. Chem.* **2008**, *19*, 125 – 132.
[32] a) B. A. Arbuzov, O. A. Erastov, G. N. Nikonov, R. P. Arshinova, I. P. Romanova, R. A. Kadyrov, *Bull. Acad. Sci. URSS* **1983**, *32*, 1672 – 1676; b) G. Märkl, G. Yu. Jin, Ch. Schoerner, *Tetrahedron Lett.* **1980**, *21*, 1409 – 1412; c) G. N. Nikonov, A. S. Balueva, O. A. Erastov, B. A. Arbuzov, *Bull. Acad. Sci. URSS* **1989**, *38*, 1223 – 1226; d) A. A. Karasik, R. N. Naumov, O. G. Sinyashin, G. P. Belov, H. V. Novikova, P. Lönnecke, E. Hey-Hawkins, *Dalton Trans.* **2003**, 2209 – 2214; e) A. Jain, S. Lense, J. Linehan, S. Raugei, H. Cho, D. L. Dubois, W. J. Shaw, *Inorg. Chem.* **2011**, *50*, 4073 – 4085; f) A. A. Karasik, G. N. Nikonov, B. A. Arbuzov, R. Z. Musin, Yu.Ya. Efremov, *Bull. Acad. Sci. URSS* **1991**, *40*, 633 – 637.
[33] A. A. Karasik, R. N. Naumov, Yu. S. Spiridonova, O. G. Sinyashin, P. Lönnecke, E. Hey-Hawkins, *Z. Anorg. Allg. Chem.* **2007**, *633*, 205 – 210.
[34] E. S. Wiedner, J. Y. Yang, W. G. Dougherty, W. S. Kassel, R. M. Bullock, M. Rakowski DuBois, D. L. DuBois, *Organometallics* **2010**, *29*, 5390 – 5401.
[35] S. N. Ignatieva, A. S. Balueva, A. A. Karasik, Sh. K. Latypov, A. G. Nikonova, O. E. Naumova, P. Lönnecke, E. Hey-Hawkins, O. G. Sinyashin, *Inorg. Chem.* **2010**, *49*, 5407 – 5412.
[36] a) Zh. V. Molodykh, N. N. Anisimova, M. A. Kudrina, M. S. Loseva, G. N. Nikonov, O. A. Erastov, *Pharm. Chem. J.* **1983**, *17*, 206 – 210; b) E. I. Musina, R. M. Kuznetsov, E. F. Gubanov, A. S. Balueva, G. N. Nikonov, *Russ. J. Gen. Chem.* **1999**, *69*, 891 – 896.
[37] A. A. Karasik, Yu. S. Spiridonova, D. G. Yakhvarov, O. G. Sinyashin, P. Lönnecke, R. Sommers, E. Hey-Hawkins, *Mendeleev Commun.* **2005**, 89 – 90.
[38] A. A. Karasik, R. N. Naumov, R. Sommer, O. G. Sinyashin, E. Hey-Hawkins, *Polyhedron* **2002**, *21*, 2251 – 2256.
[39] A. A. Karasik, I. O. Georgiev, E. I. Musina, O. G. Sinyashin, J. Heinicke, *Polyhedron* **2001**, *20*, 3321 – 3331.
[40] G. U. Spiegel, O. Stelzer, *Chem. Ber.* **1990**, *123*, 989 – 993.
[41] D. Redmore, *J. Org. Chem.* **1970**, *35*, 4114 – 4117.
[42] a) B. A. Arbuzov, O. A. Erastov, G. N. Nikonov, I. A. Litvinov, D. S. Yufit, Yu. T. Struchkov, *Bull. Acad. Sci URSS* **1981**, *30*, 1872 – 1876; b) A. A. Karasik, G. N. Nikonov, *Zh. Obshch. Khim.* **1993**, *63*, 2775 – 2790.
[43] R. M. Galimullina, M. I. Valitov, Yu. S. Spiridonova, E. I. Musina, S. A. Krasnov, M. K. Kadirov, A. A. Karasik, Yu. G. Budnikova, O. G. Sinyashin, *Russ. J. Phys. Chem. A* **2011**, *85*, 2214 – 2221.
[44] E. Lindner, R. Fawzi, H. A. Mayer, K. Eichele, W. Hiller, *Organometallics* **1992**, *11*, 1033 – 1043.
[45] P. Meier, A. E. Merbach, *J. Chem. Soc. Chem. Commun.* **1979**, 49 – 50.
[46] A. Bondi, *J. Phys. Chem.* **1964**, *68*, 441 – 444.
[47] a) G. W. Wong, J. L. Harkreader, C. A. Mebi, B. J. Frost, *Inorg. Chem.* **2006**, *45*, 6748 – 6755; b) G. Hogarth, J Kilmartin, *J. Organomet. Chem.* **2007**, *692*, 5655 – 5670; c) C.-H. Ueng, G.-Y. Shih, *Acta Crystallogr. Sect. C* **1992**, *48*, 988 – 991.
[48] M. Baacke, S. Hietkamp, S. Morton, O. Stelzer, *Chem. Ber.* **1982**, *115*, 1389 – 1398.
[49] a) A. D. Wilson, R. H. Newell, M. J. McNevin, J. T. Muckerman, M. Rakowski DuBois, D. L. DuBois, *J. Am. Chem. Soc.* **2006**, *128*, 358 – 366; b) J. Y. Yang, R. M. Bullock, W. J. Shaw, B. Twamley, K. Fraze, M. Rakowski DuBois, D. L. DuBois, *J. Am. Chem. Soc.* **2009**, *131*, 5935 – 5945.
[50] V. Fourmond, P.-A. Jacques, M. Fontecave, V. Artero, *Inorg. Chem.* **2010**, *49*, 10338 – 10347.
[51] a) G. A. N. Felton, R. S. Glass, D. L. Lichtenberger, D. H. Evans, *Inorg. Chem.* **2006**, *45*, 9181 – 9184; b) M. Wang, L. Chen, L. Sun, *Energy Environ. Sci.* **2012**, *5*, 6763 – 6778; c) J. A. S. Roberts, R. M. Bullock, *Inorg. Chem.* **2013**, *52*, 3823 – 3835.

[52] M. K. Kadirov, M. I. Valitov, I. R. Nizameev, D. M. Kadirov, Sh. N. Mirkhanov, *Russ. Chem. Bull.* **2010**, *59*, 1543 – 1548.
[53] a) R. S. Nicholson, I. Shain, *Anal. Chem.* **1964**, *36*, 706 – 723; b) J. M. Savéant, E. Vianello, *Electrochim. Acta* **1965**, *10*, 905 – 920; c) J. M. Savéant, E. Vianello, *Electrochim. Acta* **1967**, *12*, 629 – 646; d) A. Jain, M. L. Reback, M. L. Lindstrom, C. E. Thogerson, M. L. Helm, A. M. Appel, W. J. Shaw, *Inorg. Chem.* **2012**, *51*, 6592 – 6602.
[54] CrysAlis Pro: Data collection and data reduction software package, Agilent Technologies.
[55] SCALE3 ABSPACK: Empirical absorption correction using spherical harmonics.
[56] APEX2 (Version 2.1), SAINTPlus. Data Reduction and Correction Program (Version 7.31 A), Bruker Advanced X-ray Solutions, BrukerAXS Inc., Madison, Wisconsin, USA, 2006.
[57] G. M. Sheldrick, SADABS Bruker AXS Inc., **2002**.
[58] SIR92, A. Altomare, G. Cascarano, C. Giacovazzo, A. Guagliardi, *J. Appl. Crystallogr.* **1993**, *26*, 343 – 350.
[59] G. M. Sheldrick, *Acta Crystallogr. Sect. A* **2008**, *64*, 112 – 122.
[60] DIAMOND Version 3.2i: K. Brandenburg, Crystal Impact GbR, Bonn, Germany.
[61] D. Drew, J. R. Doyle, *Inorg. Synth.* **1972**, *13*, 48.
[62] J. Wiedermann, K. Mereiter, K. Kirchner, *J. Mol. Catal. A* **2006**, *257*, 67 – 72.
[63] P. W. N. M. van Leeuwen, W. L. Groeneveld, *Inorg. Nucl. Chem. Lett.* **1967**, *3*, 145 – 146.
[64] S. Pfirrmann, C. Limberg, E. Hoppe, *Z. Anorg. Allg. Chem.* **2009**, *635*, 312 – 316.

Received: October 30, 2013
Published online on February 12, 2014

